Dickinson) was employed as secondary reagents. FITC- (PharMingen, San Diego, CA), PE- (Dako Glostrup, Denmark), Per CP- (Becton Dickinson), APC- (Becton Dickinson) conjugated species- and isotype-matched, mAbs were used to determine the level of background staining.

Elispot Assay

We performed enzyme-linked immunospot (Elispot) assay to know the efficiency of HIV-1 specific T-cell induction by DCs infected with AdV or SeV vector. First, we developed mDCs as described above from PBMCs of two HIV-1-infected patients. On day 7, we infected those mDCs with AdV vector at an MOI of 1,000 or SeV vector at an MOI of 2 for 1 hr, or just added overlapping peptides (*gag*, *env*). We used the overlapping peptides derived from consensus B sequence since both patients were infected with subtype B HIV-1. We did not check the AdV sero-status of these two patients. Both patients were on HAART and have undetectable viral load (<50 copies/ml). CD4 counts of patients 1 and 2 are 408/μl and 336/μl, respectively. We used those mDCs as stimulators in Elispot assay. PBMCs from each patient were used as effectors cells. The protocol of Elispot assay was described previously [Furutsuki et al., 2004].

RESULTS

Sendai Viral Vectors Transduce DCs at Lower MOIs Than Adenoviral Vectors

We infected imDCs with SeVGFP, dF-SeVGFP or AdVGFP at different MOIs (Fig. 1) in order to know which MOI is the best for these three vectors. We stained these cells with PI to evaluate the expression of GFP in viable cells. In SeVGFP, the expression of GFP reached the maximum (32.5%) at an MOI of 2 and the mean fluorescent intensity (MFI) of GFP showed around 1,400 at all MOIs. However, as shown by the fraction of PI-positive cells, SeVGFP killed around 30% of DCs even at an MOI of 0.5. The staining pattern of DCs infected with dF-SeVGFP was similar to that of SeVGFP. In AdVGFP, both the percentage of GFP-positive cells and the MFI of

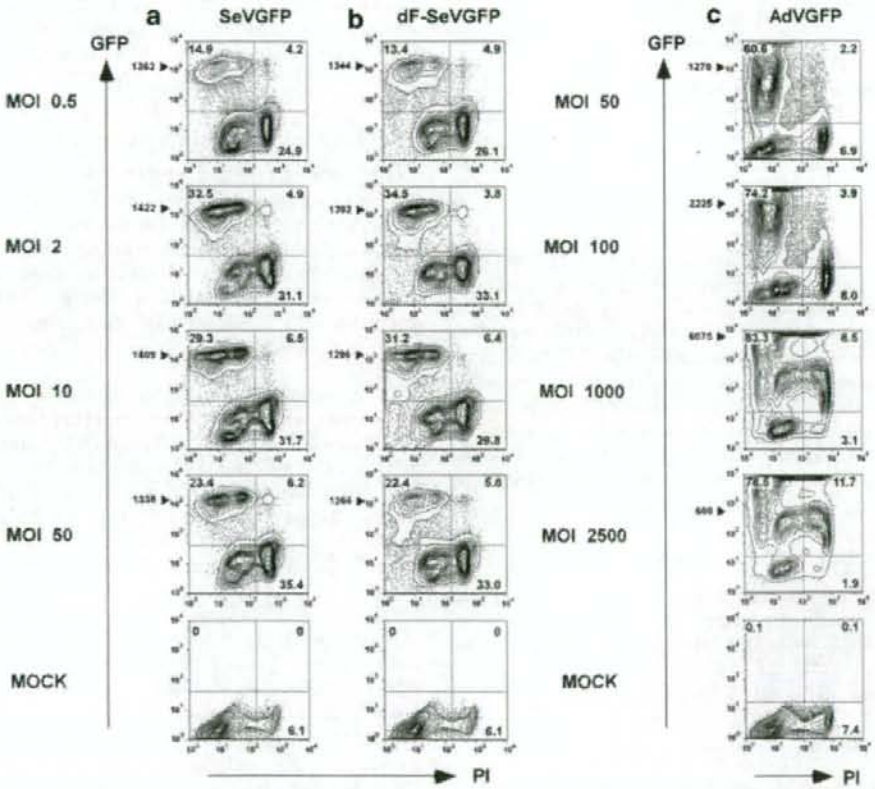

Fig. 1. Comparison of different MOIs for the maximum gene expression by SeV (**a**), dF-SeV (**b**), and AdV (**c**) vectors 48 hr after infection. Cell viability was determined by staining with PI. GFP expression and PI staining were analyzed by flow cytometry. The percentages of GFP- and PI-positive cells are shown on each corner. Arrowheads indicate MFI of GFP-positive cells within PI-negative fraction. The numbers in each panel represent the mean value of three independent experiments.

GFP increased up to an MOI of 1,000. Although PI-positive cells in AdV increased according to MOIs, the percentage of PI-positive cells was less than 14% even at the highest MOI: 2,500. From these results, SeV vector is likely to transduce DCs at much lower MOIs than AdV vector, but kill more DCs than AdV. We chose an MOI of 2 for SeVGFP and dF-SeVGFP, and an MOI of 1,000 for AdVGFP in the subsequent experiments.

Sendai Viral Vectors Showed Maximum Transduction Level Earlier Than Adenoviral Vectors

We next examined the time course of GFP expression (Fig. 2). We detected GFP-positive cells as early as 8 hr after infection in all three vectors. The proportion of GFP-positive cells reached the maximum level (around

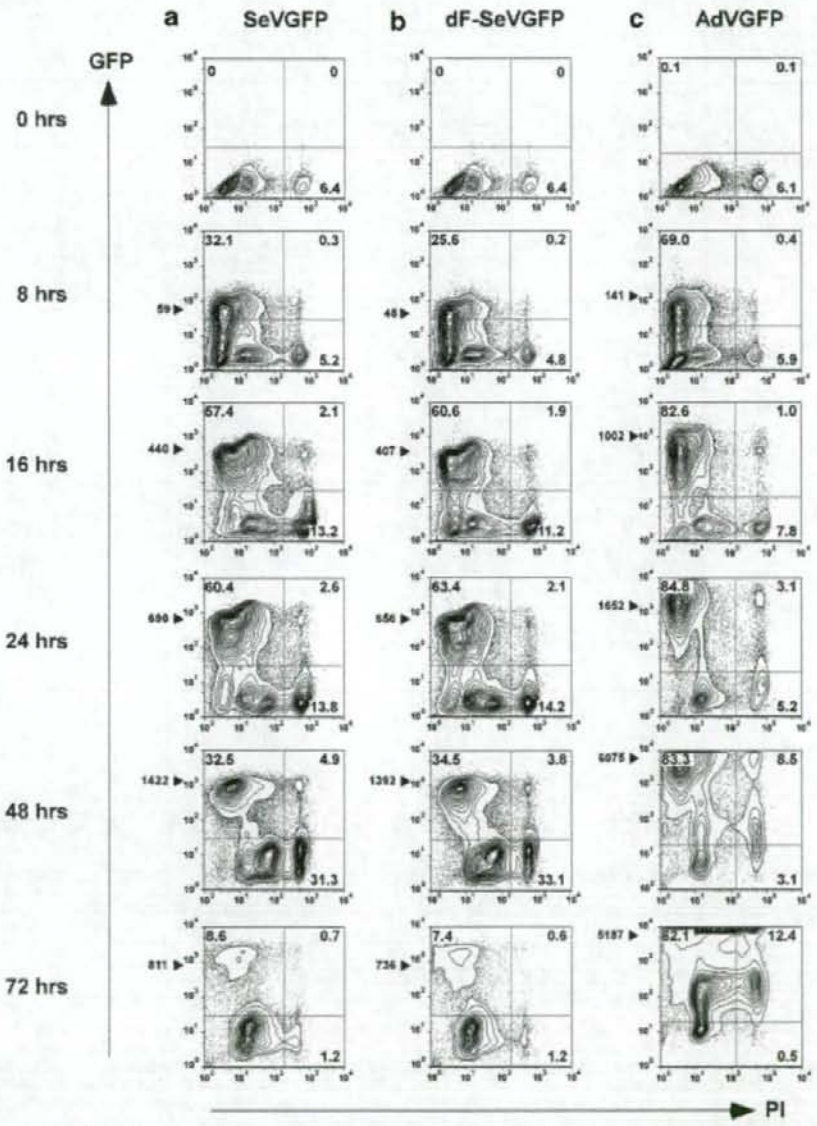

Fig. 2. The time course of the maximum gene expression by SeV (a), dF-SeV (b), and AdV (c) vectors. DCs were infected with SeV and dF-SeV at an MOI of 2 and were infected with AdV at MOI of 1,000 and then cultured for 8–72 hr. Cell viability was determined by staining with PI. GFP expression and PI staining were analyzed by flow cytometry. The percentages of GFP- and PI-positive cells are shown on each corner. Arrowheads indicate MFI of GFP-positive cells within PI-negative fraction. The numbers in each panel represent the mean value of three independent experiments.

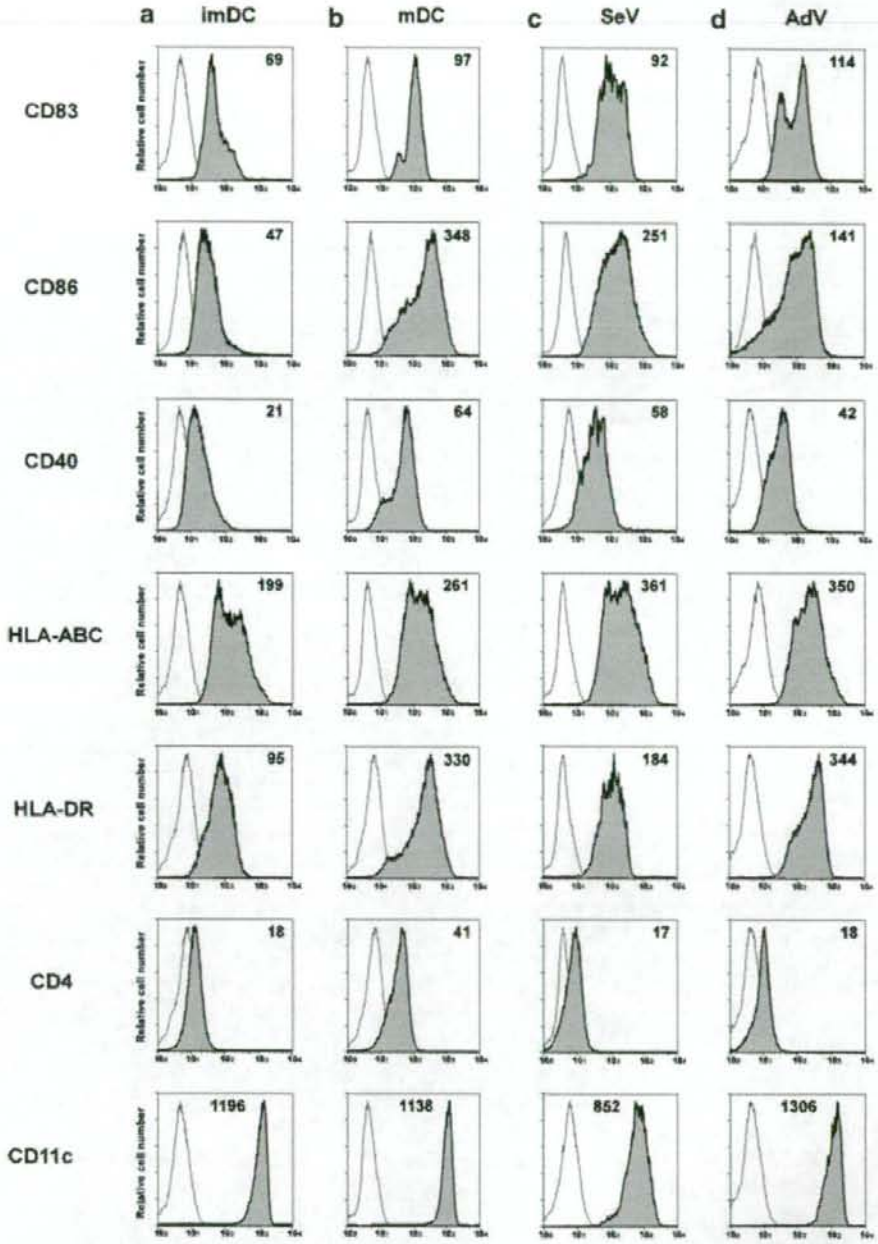

Fig. 3. Infection of DCs with SeV and AdV vectors modified the expression of cell surface markers. DCs infected with SeV vector containing no inserts at an MOI of 2 (**c**) and AdV vector containing no inserts at an MOI of 1,000 (**d**) were maintained in the DC medium for 48 hr (AdV vector) and 24 hr (SeV vector). DCs were incubated with (**b**) or without (**a**) TNF-α for 48 hr, respectively. These DCs were analyzed by flow cytometry with FITC, PE, PerCP, APC-conjugated antibodies for expression of CD86, CD83, HLA-ABC, HLA-DR, CD4, CD40, CD11c. The open profiles represent isotype-matched mAb controls. MFIs are indicated on the right corner in each panel. The background values of all experiments were less than 15. The numbers in each panel represent the mean value of three independent experiments.

60%) 24 hr after infection with SeVGFP or dF-SeVGFP. The proportion of GFP-positive cells decreased to around 30% at 48 hr, although the MFI of GFP showed the maximum at 48 hr. AdVGFP, on the other hand, showed the maximum level of both GFP-positive cells and MFI of GFP 48 hr after infection.

Sendai and Adenoviral Vectors Changed Phenotype of imDCs Following Viral Transduction

In order to determine the effect of transduction on imDCs with these vectors, we examined the surface markers of cells after transduction. The phenotype of imDCs and mDCs are shown in Figure 3a,b, respectively. We infected imDCs with SeV or AdV vectors and cultured them for 24 or 48 hr, respectively (Fig. 3c,d). As compared with the phenotype of uninfected imDCs, DCs infected by SeV and AdV vectors showed up-regulation of a maturation marker CD83, the major histocompatibility complex (MHC) classes I and II molecules (HLA-ABC and HLA-DR), and costimulatory molecules CD40 and CD86. Incubation of DCs in medium and buffers used to prepare vectors did not affect the phenotype of the cells (data not shown). These results indicate that SeV as well as AdV vector infection induced DC maturation in terms of cell surface phenotype.

Both SeV and AdV Vectors Elicited HIV-1 Specific T-Cell Responses

To evaluate protein expressions, we developed five viral vectors carrying HIV-1 structural proteins (Fig. 4a). We infected DCs with these vectors under the optimal conditions we concluded from the results shown above. Gp120 expression by SeV vector was 3.8 times higher than that by AdV vector (Fig. 4b, compare lanes 3–7). Since 3.2 and 5.0 kb are the maximum gene sizes for SeV and AdV vector, respectively [Sakai et al., 1999; the manufacturer's protocol of AdV Expression Kit], we inserted HIV-1 *gag* gene (about 1.5 kb) in SeV and *gag-pol* gene (about 4.9 kb) in AdV vector. Both *cis*-acting RRE sequence and *trans*-acting Rev protein were necessary for Gag protein expression by AdV vector (Fig. 4b, compare lanes 1–2). Rev expression is not required for SeV-mediated Gag or Env expression because SeV replicates in the cytoplasm. In the presence of Rev protein, AdV vector expressed similar levels of Gag protein to SeV vector (Fig. 4b, compare lanes 1–6). Although SeV Gag did not have HIV-1 protease sequence, a band was detected near the size of p24. It was not a nonspecific band derived from SeV because we could not detect the band with other SeV constructs, such as SeV Env (data not shown). Gag might be processed by some proteins of SeV.

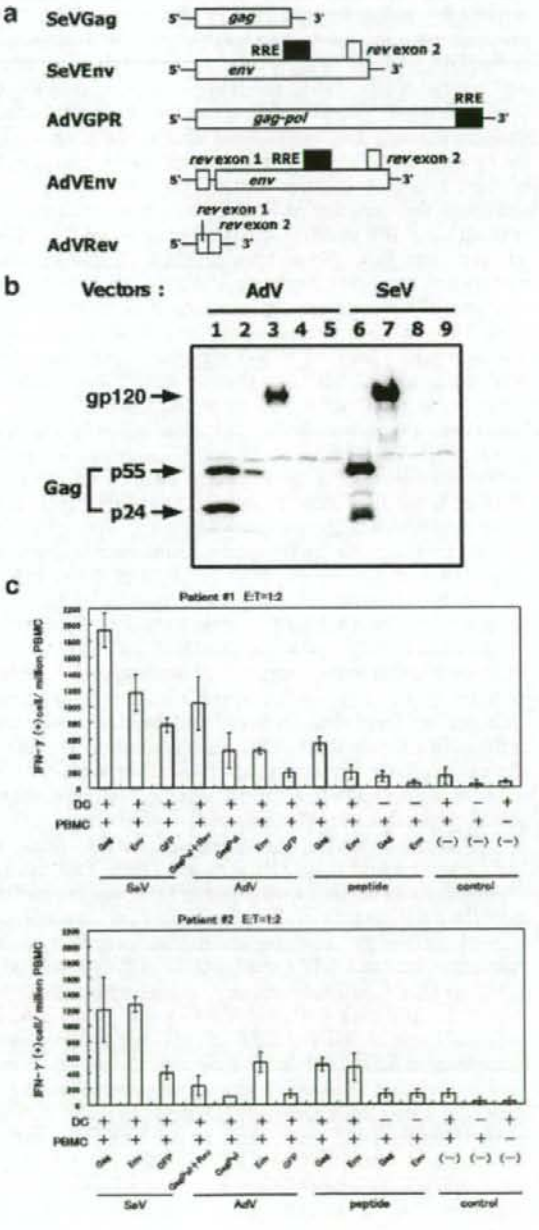

Fig. 4. **a**: Schematic structures of five viral vectors. *gag*, HIV-1 gag gene; *env*, HIV-1 env gene; *gag-pol*, HIV-1 gag and pol genes; *rev*, HIV-1 rev gene; RRE, HIV-1 RRE; GFP, green fluorescent protein. **b**: The expression of HIV-1 structural proteins by AdV and SeV vectors. DCs infected with AdV vector at an MOI of 1,000 and SeV vector at an MOI of 2 were harvested for 48 or 24 hr after infection, respectively. Thirty microgram of lysate was subjected to immunoblot analysis using anti-Gag p24 or anti-Env gp120 mAbs. The other two independent experiments showed similar results. Lane 1, coinfection with AdVGPR and AdVRev; Lane 2, AdVGPR without AdVRev infection; Lane 3, AdVEnv; Lane 4, AdV without inserts; Lane 5, mock; Lane 6, SeVGag; Lane 7, SeVEnv; Lane 8, SeV without inserts; Lane 9, mock. Arrows on the left indicate positions of gp120, Gag p55, and p24. **c**: The results of IFN-γ Elispot assays in two HIV-1 infected patients. Autologous DCs infected with SeV vector or AdV vector, or just added overlapping peptides (*gag*, *env*) were used as stimulators. PBMCs from the same patients were used as effectors cells. Results are shown as mean ± SEM of three independent assays.

After developing mDCs from frozen PBMCs of two HIV-1 infected patients, we infected these mDCs with SeV or AdV vector and used them as stimulators for interferon γ (IFN-γ) Elispot. Both SeV and AdV vectors elicited HIV-1 specific T-cell responses, although some nonspecific responses were also detected (Fig. 4c).

DISCUSSION

DCs are efficient antigen presenting cells that are critical for induction of primary T-cell responses. At present the most useful method for genetic manipulation of DCs is to use viral vectors. As reported previously, AdV vector is efficient at the transduction of DCs [Tan et al., 2005]. SeV is also one of the reliable vectors for immunotherapy and has several unique features, such as cytoplasmic localized replication cycle and brief contact time for cellular uptake. In this study, we analyzed the capacity of SeV as a vector in terms of transducing GFP and HIV-1 genes into human DCs. We showed that SeV vector transduced GFP genes efficiently into monocyte-derived imDCs. DCs infected with SeV and dF-SeV vectors expressed high amount of GFP gene 24 hr after infection at an MOI of 2 (Fig. 2a,b). The expression level of HIV-1 structural gene, *env*, by SeV vector was higher than that by AdV. These results proved the high ability of gene expression by SeV. However, the proportion of GFP positive cells did not increase according to MOI. About 30% of cells were still GFP-negative 48 hr after infection even at an MOI of 50 (Fig. 1a,b). This could be caused by the disruption of sialic acid which is the receptor for SeV.

Both SeV and dF-SeV vectors killed nearly 30% of target DCs at the lowest MOI: 0.5. One of the reasons for this phenomenon is likely to be apoptosis. Several studies reported that SeV is able to induce apoptosis in viral host cells [Tropea et al., 1995; Bitzer et al., 1999]. This cytopathic effect might enhance specific T-cell responses by cross-presentation of DCs. Presentation by DCs derived from virus-infected apoptotic and necrotic cells could activate T-cells efficiently [Arrode et al., 2000; Herr et al., 2000; Larsson et al., 2001; Tabi et al., 2001]. In order to apply SeV in a clinical setting, further studies about cytopathic effect by SeV vector will be required.

AdV vector is known to require high MOI to achieve high transduction rates [Diao et al., 1999]. Our study also demonstrated that much higher MOI was needed in AdV than SeV to transduce DCs. One of the reasons for this phenomenon could be insufficient expression of coxsackievirus and AdV receptor (CAR) [Stockwin et al., 2002] on DCs. CAR is the primary receptor for AdV type 5, and the AdV used in this study was derived from AdV type 5. However, MFI of GFP in AdV vector increased according to MOI. AdV might be able to use other receptors to infect DCs. Several studies have shown that AdV can infect cells through integrins or MHC molecules [Huang et al., 1996; Hong et al., 1997]. Recently, AdV vector containing Ad5/35 chimeric fiber protein was reported as a useful vector for the cells lacking in sufficient CAR expression [Mizuguchi and Hayakawa, 2002]. This chimeric vector would be useful for DCs because the receptor of Ad5/35 vector is CD46, which is expressed on DCs.

When imDCs capture antigens, they maturate while migrating to T-cell areas in the lymph nodes [Banchereau and Steinman, 1998]. DC maturation is critical for strong T-cell binding and stimulation [Lipscomb and Masten, 2002]. Our results showed that SeV vector infection induced DC maturation of human monocyte-derived DCs as well as AdV vector infection. However, the expression levels of CD86 and CD40 were lower as compared to those of mDCs. CD40 expression leads to increased DC survival and stimulates cytokine production [Caux et al., 1994; Wong et al., 1997]. CD86, a ligand for CD28 and cytotoxic T-lymphocyte-associated protein 4 (CTLA-4), stimulates T-cell proliferation and generation of CTL [Lanier et al., 1995]. In order to achieve further up-regulation of those molecules, the addition of a maturation factor, such as TNF-α, should be considered.

DCs infected with SeV as well as AdV elicited HIV-1 specific T-cell responses detected by IFN-γ Elispot (Fig. 4c). Elispot by SeV GFP showed about 800 SFC/million PBMC which was obtained from patient #1. One possibility of this nonspecific response is antigenic cross-reactivity. SeV belongs to the genus *Respirovirus* of the *Paramyxoviridae* family. *Respirovirus* includes human parainfluenza virus type 1 (hPIV-1) and 3 (hPIV-3). hPIV-1 is the most common cause of pediatric laryngotracheobronchitis (croup), which means many people are infected by hPIV-1 in early life. Previous studies showed SeV and hPIV-1 shared sequence homology and antigenic cross-reactivity [Gorman et al., 1990; Lyn et al., 1991; Smith et al., 1994]. The high nonspecific response by SeV GFP could be caused by cross-reactive immunity induced by previous exposure to human hPIV-1.

In conclusion, our results showed that SeV vector had high ability of gene transduction. SeV vector induced the maturation of DCs in terms of their phenotype and stimulated HIV-1 specific T-cell responses, which is beneficial in vaccination. Though further studies will be required to improve vector design, SeV vector has a potential to be used for immuno-genetherapy.

ACKNOWLEDGMENTS

We thank Dr. Izumu Saito and Dr. Yumi Kanegae (University of Tokyo, Japan) for providing AdVGFP and Ax1w1. This work was partly supported by grants for AIDS Research from the Ministry of Health, Labor and Welfare of Japan, The Special Coordination Fund for Promoting Science and Technology of MEXT: Strategic cooperation of control emerging and reemerging infections. This work was supported in part by the Program of Founding Research Centers for Emerging and Reemerging Infectious Diseases of the Ministry of Education, Culture, Sports, Science and Technology (MEXT); Strategic cooperation to control emerging and reemerging infections funded by the Special Coordination Funds for Promoting Science and Technology of MEXT;

(Grants for Research on HIV/AIDS and Research on Publicly Essential Drugs and Medical Devises from the Ministry of Health, Labor, and Welfare of Japan; Grant-in-Aid for Scientific Research (B) from Japan Society for the Promotion of Science (JSPS).

REFERENCES

Agungpriyono DR, Yamaguchi R, Uchida K, Tohya Y, Kato A, Nagai Y, Asakawa M, Tateyama S. 2000. Green fluorescent protein gene insertion of Sendai Virus infection in nude mice: Possibility as an infection tracer. J Vet Med Sci 62:223–228.

Arrode G, Boccaccio C, Lule J, Allart S, Moinard N, Abastado JP, Alam A, Davrinche C. 2000. Incoming human cytomegalovirus pp65 (UL83) contained in apoptotic infected fibroblasts is cross-presented to CD8(+) T cells by dendritic cells. J Virol 74:10018–10024.

Banchereau J, Steinman RM. 1998. Dendritic cells and the control of immunity. Nature 392:245–252.

Bitzer M, Prinz F, Bauer M, Spiegel M, Neubert WJ, Gregor M, Schulze-Osthoff K, Lauer U. 1999. Sendai virus infection induces apoptosis through activation of caspase-8 (FLICE) and caspase-3 (CPP32). J Virol 73:702–708.

Bonini C, Lee SP, Riddell SR, Greenberg PD. 2001. Targeting antigen in mature dendritic cells for simultaneous stimulation of CD4+ and CD8+ T cells. J Immunol 166:5250–5257.

Brander C, Walker BD. 1999. T lymphocyte responses in HIV-1 infection: Implications for vaccine development. Curr Opin Immunol 11:451–459.

Caux C, Massacrier C, Vanbervliet B, Dubois B, Van Kooten C, Durand I, Banchereau J. 1994. Activation of human dendritic cells through CD40 cross-linking. J Exp Med 180:1263–1272.

Diao J, Smythe JA, Smyth C, Rowe PB, Alexander IE. 1999. Human PBMC-derived dendritic cells transduced with an adenovirus vectorinduce cytotoxic T-lym-phocyte responses against a vector-encoded antigen in vitro. Gene Ther 6:845–853.

Engelmayer J, Larsson M, Subklewe M, Chahroudi A, Cox WI, Steinman RM, Bhardwaj N. 1999. Vaccinia virus inhibits the maturation of human dendritic cells: A novel mechanism of immune evasion. J Immunol 163:6762–6768.

Engelmayer J, Larsson M, Lee A, Lee M, Cox WI, Steinman RM, Bhardwaj N. 2001. Mature dendritic cells infected with canarypox virus elicit strong anti-human immunodeficiency virus CD8+ and CD4+ T-cell responses from chronically infected individuals. J Virol 75:2142–2153.

Furutsuki T, Hosoya N, Kawana-Tachikawa A, Tomizawa M, Odawara T, Goto M, Kitamura Y, Nakamura T, Kelleher AD, Cooper DA, Iwamoto A. 2004. Frequent transmission of cytotoxic-T-lymphocyte escape mutants of human immunodeficiency virus type 1 in the highly HLA-A24-positive Japanese population. J Virol 78:8437–8445.

Gorman WL, Gill DS, Scroggs RA, Portner A. 1990. The hemagglutinin-neuraminidase glycoproteins of human parainfluenza virus type 1 and Sendai virus have high structure-function similarity with limited antigenic cross-reactivity. Virology 175:211–221.

Graham FL, Smiley J, Russell WC, Nairn R. 1977. Characteristics of a human cell line transformed by DNA from human adenovirus type 5. J Gen Virol 36:59–74.

Herr W, Ranieri E, Olson W, Zarour H, Gesualdo L, Storkus WJ. 2000. Mature dendritic cells pulsed with freeze-thaw cell lysates define an effective in vitro vaccine designed to elicit EBV-specific CD4(+) and CD8(+) T lymphocyte responses. Blood 96:1857–1864.

Hong SS, Karayan L, Tournier J, Curiel DT, Boulanger PA. 1997. Adenovirus type 5 fiber knob binds to MHC class I alpha2 domain at the surface of human epithelial and B lymphoblastoid cells. EMBO J 16:2294–2306.

Huang S, Kamata T, Takada Y, Ruggeri ZM, Nemerow GR. 1996. Adenovirus interaction with distinct integrins mediates separate events in cell entry and gene delivery to hematopoietic cells. J Virol 70:4502–4508.

Ishii-Watabe A, Uchida E, Iwata A, Nagata R, Satoh K, Fan K, Murata M, Mizuguchi H, Kawasaki N, Kawanishi T, Yamaguchi T, Hayakawa T. 2003. Detection of replication-competent adenoviruses spiked into recombinant adenovirus vector products by infectivity PCR. Mol Ther 8:1009–1016.

Jin X, Bauer DE, Tuttleton SE, Lewin S, Gettie A, Blanchard J, Irwin CE, Safrit JT, Mittler J, Weinberger L, Kostrikis LG, Zhang L, Perelson AS, Ho DD. 1999. Dramatic rise in plasma viremia after CD8(+) T cell depletion in simian immunodeficiency virus-infected macaques. J Exp Med 189:991–998.

Kanegae Y, Makimura M, Saito I. 1994. A simple and efficient method for purification of infectious recombinant adenovirus. Jpn J Med Sci Biol 47:157–166.

Kano M, Matano T, Kato A, Nakamura H, Takeda A, Suzaki Y, Ami Y, Terao K, Nagai Y. 2002. Primary replication of a recombinant Sendai virus vector in macaques. J Gen Virol 83:1377–1386.

Kato A, Sakai Y, Shioda T, Kondo T, Nakanishi M, Nagai Y. 1996. Initiation of Sendai virus multiplication from transfected cDNA or RNA with negative or positive sense. Genes Cells 1:569–579.

Kato M, Igarashi H, Takeda A, Sasaki Y, Nakamura H, Kano M, Sata T, Iida A, Hasegawa M, Horie S, Higashihara E, Nagai Y, Matano T. 2005. Induction of Gag-specific T-cell responses by therapeutic immunization with a Gag-expre-ssing Sendai virus vector in macaques chronically infected with simian-human immunodeficiency virus. Vaccine 23:3166–3173.

Kawana-Tachikawa A, Tomizawa M, Nunoya J, Shioda T, Kato A, Nakayama EE, Nakamura T, Nagai Y, Iwamoto A. 2002. An efficient and versatile mammalian viral vector system for major histocompatibility complex class I/peptide complexes. J Virol 76: 11982–11988.

Lanier LL, O'Fallon S, Somoza C, Phillips JH, Linsley PS, Okumura K, Ito D, Azuma M. 1995. CD80 (B7) and CD86 (B70) provide similar costimulatory signals for T cell proliferation, cytokine production, and generation of CTL. J Immunol 154:97–105.

Larsson M, Fonteneau JF, Somersan S, Sanders C, Bickham K, Thomas EK, Mahnke K, Bhardwaj N. 2001. Efficiency of cross presentation of vaccinia virus-derived antigens by human dendritic cells. Eur J Immunol 31:3432–3442.

Levy JA, Cheng-Mayer C, Dina D, Luciw PA. 1986. AIDS retrovirus (ARV-2) clone replicates in transfected human and animal fibroblasts. Science 232:998–1001.

Li HO, Zhu YF, Asakawa M, Kuma H, Hirata T, Ueda Y, Lee YS, Fukumura M, Iida A, Kato A, Nagai Y, Hasegawa M. 2000. A cytoplasmic RNA vector derived from nontransmissible Sendai virus with efficient gene transfer and expression. J Virol 74:6564–6569.

Lipscomb MF, Masten BJ. 2002. Dendritic cells: Immune regulators in health and disease. Physiol Rev 82:97–130.

Lyn D, Gill DS, Scroggs RA, Portner A. 1991. The nucleoproteins of human parainfluenza virus type 1 and Sendai virus share amino acid sequences and antigenic and structural determinants. J Gen Virol 72:983–987.

Matano T, Shibata R, Siemon C, Connors M, Lane HC, Martin MA. 1998. Administration of an anti-CD8 monoclonal antibody interferes with the clearance of chimeric simian/human immunodeficiency virus during primary infections of rhesus macaques. J Virol 72:164–169.

McMichael AJ, Rowland-Jones SL. 2001. Cellular immune responses to HIV. Nature 410:980–987.

Miyake S, Makimura M, Kanegae Y, Harada S, Sato Y, Takamori K, Tokuda C, Saito I. 1996. Efficient generation of recombinant adenoviruses using adenovirus DNA-terminal protein complex and a cosmid bearing the full-length virus genome. Proc Natl Acad Sci USA 93:1320–1324.

Mizuguchi H, Hayakawa T. 2002. Adenovirus vectors containing chimeric type 5 and type 35 fiber proteins exhibit altered and expanded tropism and increase the size limit of foreign genes. Gene 285:69–77.

Mwau M, Cebere I, Sutton J, Chikoti P, Winstone N, Wee EG, Beattie T, Chen YH, Dorrell L, McShane H, Schmidt C, Brooks M, Patel S, Roberts J, Conlon C, Rowland-Jones SL, Bwayo JJ, McMichael AJ, Hanke T. 2004. A human immunodeficiency virus 1 (HIV-1) clade A vaccine in clinical trials: Stimulation of HIV-specific T-cell responses by DNA and recombinant modified vaccinia virus Ankara (MVA) vaccines in humans. J Gen Virol 85: 911–919.

Nagayama H, Sato K, Morishita M, Uchimaru K, Oyaizu N, Inazawa T, Yamasaki T, Enomoto M, Nakaoka T, Nakamura T, Maekawa T, Yamamoto A, Shimada S, Saida T, Kawakami Y, Asano S, Tani K, Takahashi TA, Yamashita N. 2003. Results of a phase I clinical study using autologous tumour lysate-pulsed monocyte-derived mature dendritic cell vaccinations for stage IV malignant mela-

noma patients combined with low dose interleukin-2. Melanoma Res 13:521–530.

Rea D, Schagen FH, Hoeben RC, Mehtali M, Havenga MJ, Toes RE, Melief CJ, Offringa R. 1999. Adenoviruses activate human dendritic cells without polarization toward a T-helper type 1-inducing subset. J Virol 73:10245–10253.

Rouas R, Uch R, Cleuter Y, Jordier F, Bagnis C, Mannoni P, Lewalle P, Martiat P, Van den Broeke A. 2002. Lentiviral-mediated gene delivery in human monocyte-derived dendritic cells: Optimized design and procedures for highly efficient transduction compatible with clinical constraints. Cancer Gene Ther 9:715–724.

Sakai Y, Kiyotani K, Fukumura M, Asakawa M, Kato A, Shioda T, Yoshida T, Tanaka A, Hasegawa M, Nagai Y. 1999. Accommodation of foreign genes into the Sendai virus genome: Sizes of inserted genes and viral replication. FEBS Lett 456:221–226.

Smith FS, Portner A, Leggiadro RJ, Turner EV, Hurwitz JL. 1994. Age-related development of human memory T-helper and B-cell responses toward parainfluenza virus type-1. Virology 205:453–461.

Stockwin LH, Matzow T, Georgopoulos NT, Stanbridge LJ, Jones SV, Martin IG, Blair-Zajdel ME, Blair GE. 2002. Engineered expression of the Coxsackie B and adenovirus receptor (CAR) in human dendritic cells enhances recombinant adenovirus-mediated gene transfer. J Immunol Methods 259:205–215.

Stubbs AC, Martin KS, Coeshott C, Skaates SV, Kuritzkes DR, Bellgrau D, Franzusoff A, Duke RC, Wilson CC. 2001. Whole recombinant yeast vaccine activates dendritic cells and elicits protective cell-mediated immunity. Nat Med 7:625–629.

Tabi Z, Moutaftsi M, Borysiewicz LK. 2001. Human cytomegalovirus pp65- and immediate early 1 antigen-specific HLA class I-restricted cytotoxic T cell responses induced by cross-presentation of viral antigens. J Immunol 166:5695–5703.

Takeda A, Igarashi H, Nakamura H, Kano M, Iida A, Hirata T, Hasegawa M, Nagai Y, Matano T. 2003. Protective efficacy of an AIDS vaccine, a single DNA priming followed by a single booster with a recombinant replication-defective Sendai virus vector, in a macaque AIDS model. J Virol 77:9710–9715.

Tan PH, Beutelspacher SC, Xue SA, Wang YH, Mitchell P, McAlister JC, Larkin DF, McClure MO, Stauss HJ, Ritter MA, Lombardi G, George AJ. 2005. Modulation of human dendritic-cell function following transduction with viral vectors: Implications for gene therapy. Blood 105:3824–3832.

Tropea F, Troiano L, Monti D, Lovato E, Malorni W, Rainaldi G, Mattana P, Viscomi G, Ingletti MC, Portolani M, et al. 1995. Sendai virus and herpes virus type 1 induce apoptosis in human peripheral blood mononuclear cells. Exp Cell Res 218:63–70.

Tsunetsugu-Yokota Y, Morikawa Y, Isogai M, Kawana-Tachikawa A, Odawara T, Nakamura T, Grassi F, Autran B, Iwamoto A. 2003. Yeast-derived human immunodeficiency virus type 1 p55(gag) virus-like particles activate dendritic cells (DCs) and induce perforin expression in Gag-specific CD8(+) T cells by cross-presentation of DCs. J Virol 77:10250–10259.

Wong BR, Josien R, Lee SY, Sauter B, Li HL, Steinman RM, Choi Y. 1997. TRANCE (tumor necrosis factor [TNF]-related activation-induced cytokine), a new TNF family member predominantly expressed in T cells, is a dendritic cell-specific survival factor. J Exp Med 186:2075–2080.

Yang OO, Kalams SA, Trocha A, Cao H, Luster A, Johnson RP, Walker BD. 1997. Suppression of human immunodeficiency virus type 1 replication by CD8+ cells: Evidence for HLA class I-restricted triggering of cytolytic and noncytolytic mechanisms. J Virol 71: 3120–3128.

Yu D, Shioda T, Kato A, Hasan MK, Sakai Y, Nagai Y. 1997. Sendai virus-based expression of HIV-1 gp120: Reinforcement by the V(−) version. Genes Cells 2:457–466.

Erythromycin derivatives inhibit HIV-1 replication in macrophages through modulation of MAPK activity to induce small isoforms of C/EBPβ

Iwao Komuro*†, Toshiaki Sunazuka‡, Kiyoko S. Akagawa*‡, Yasuko Yokota*, Aikichi Iwamoto†, and Satoshi Ōmura‡§

*Department of Immunology, National Institute of Infectious Diseases, 1-23-1 Toyama, Shinjuku-ku, Tokyo 162-8640, Japan; †Division of Infectious Diseases, Advanced Clinical Research Center, Institute of Medical Science, University of Tokyo, 4-6-1 Shirogandai, Minato-ku, Tokyo 108-8639, Japan; and ‡Kitasato Institute for Life Sciences, Kitasato University and the Kitasato Institute, 5-9-1 Shirokane, Minato-ku, Tokyo 108-8641, Japan

Contributed by Satoshi Ōmura, June 18, 2008 (sent for review January 11, 2008)

Macrophages (MΦs) are a major source of HIV-1 especially in patients with tuberculosis. There are MΦs that are permissive and those that restrict HIV-1. Regulation of hematopoietic cell kinase (Hck) activity and selective expression of CCAAT enhancer binding protein β (C/EBPβ) isoforms greatly contribute to determine distinct susceptibility of MΦs to HIV-1. Resistance is attributable to reduced expression of Hck and augmented expression of an inhibitory small isoform of C/EBPβ. Derivatives of erythromycin A (EMA) EM201 and EM703 inhibit the replication of HIV-1 in tissue MΦs, at posttranscriptional and translational levels. We demonstrate that EM201 and EM703 convert tissue MΦs from HIV-1 susceptible to HIV-1 resistant through down-regulation of Hck and induction of small isoforms of C/EBPβ. These drugs inhibit p38MAPK activation which is expressed only in susceptible tissue MΦs. Activated CD4$^+$T cells stimulate the viral replication in HIV-1 resistant MΦs through down-regulation of small isoforms of C/EBPβ via activation of ERK1/2. EM201 and EM703 can inhibit the MAPK activation and inhibit the burst of viral replication produced when CD4$^+$T cells and MΦs interact. These EM derivatives may be highly beneficial for repression of residual HIV-1 in the lymphoreticular system of HIV-1-infected patients and offer great promise for the creation of new anti-HIV drugs for the future treatment of AIDS patients.

AIDS | macrolides | Hck

At least 65 million people have been infected with HIV and AIDS has killed 25 million people since 1981. By 2007, worldwide, 39.5 million individuals were living with HIV, with 4.3 million new infections and 2.9 million deaths occurring in 2006 (http://data.unaids.org/pub/EpiReport/2006/02-Global_Summary_2006_EpiUpdate_eng.pdf). In developed countries, anti-HIV-1 therapy—highly active antiretroviral therapy (HAART)— potently inhibits HIV-1 replication, reduces viral antigenemia, and prolongs the survival of patients (1, 2). In contrast, patients in developing countries generally cannot use HAART therapy because of its high cost and the sheer number of patients. Furthermore, HAART therapy cannot remove HIV-1-infected latent memory T cells and monocytes (Mos)/macrophages (MΦs) in some lymphoreticular tissue, residual cells having the potential to become a viral resource capable of spreading new viral particles (3, 4). Therefore, the development of new drugs to improve and extend HAART therapy, particularly in countries in the developing world, is greatly and urgently needed.

Mos/MΦs are a major target of HIV-1 infection and serve as a reservoir for viral persistence and a chronic source of infectious virus *in vivo* (5). Most tissue MΦs are permissive to M-tropic virus entry and release a small number of virus particles in the asymptomatic carrier but they occasionally produce a large number of viral particles in the AIDS patients or HIV-1 patients with pulmonary tuberculosis (TB) or those whose conditions are complicated with opportunistic infection (3). TB markedly increases HIV-1 replication and mutation in the lung and is associated with an acceleration of AIDS (6, 7). The alveolar MΦ is the major cell type in which HIV-1 replication occurs during TB (8, 9). Thus MΦ is a key factor in the control of HIV-1 suffering.

We and others have previously demonstrated that expression of tyrosine kinase hematopoietic cell kinase (Hck) and relative amounts of a large isoform (37-kDa) to a small isoform (23-kDa) (L/S ratio) of transcription factor CCAAT enhancer binding protein β (C/EBPβ) play critical roles in M-tropic HIV-1 production in tissue MΦs (8, 10–13). We have also reported that modulation of the expression of Hck and the L/S ratio of C/EBPβ by treatment with antisense oligonucleotides can convert the phenotype of HIV-1 suceptibility in MΦs (10). These studies suggest that, not only anti-HIV-1 drugs that directly affect the virus (such as RT inhibitor or protease inhibitors), but also drugs that can convert the phenotype of tissue MΦs from "susceptible" to "resistant" by down-regulating the expression of Hck and enhancing the expression of small isoforms of C/EBPβ may be useful to help control HIV-1 replication in AIDS patients.

Macrolides with a 14-membered ring structure, such as erythromycin A (EMA), clarithromycin (CAM), or roxithromycin (RXM), are well known antibacterial drugs. Recently, these antibiotics have been shown to be efficacious against incurable chronic inflammatory airway disease, such as diffuse panbronchiolitis (DPB) (14, 15). This therapeutic efficacy is thought to be caused by either anti-inflammatory or immunomodulatory activity of the macrolide antibiotics, which can act on many cells, including epithelial cells, neutrophiles, monocytes/MΦs, and T cells (16–23). On the basis of this knowledge, we chemically modified EMA to obtain derivatives with both stronger capability for promoting monocyte-to-MΦ differentiation and no antibacterial activity. Among the derivatives, 8,9-anhydroerythromycin A 6,9-hemiketal (EM201), obtained by mild acid treatment of EMA, already known as an internal metabolite of EMA, showed a strong promotional effect on MΦ differentiation and possessed weak antimicrobial activity (24). Furthermore, the 12-membered pseudoerythromycin A (EM703) was both remarkably active and free of any antibacterial activity (25) and was known to exhibit a prophylactic effect on lung injury *in vivo* against a bleomycin-induced acute lung injury in the rat model, similar to EMA (26).

In this study, we show that both EM201 and EM703 are good lead candidates for drugs that can inhibit M-tropic HIV-1 replication in tissue MΦs by a new way of converting their phenotype from HIV-1-susceptible to HIV-1-resistant, through down-regulation of Hck and the induction of small isoforms of C/EBPβ via modulation of the activation of MAPKs.

Author contributions: T.S., K.S.A., and S.Ō. designed research; I.K., T.S., and K.S.A. performed research; T.S., Y.Y., and S.Ō. contributed new reagents/analytic tools; I.K., T.S., K.S.A., A.I., and S.Ō. analyzed data; and I.K., T.S., K.S.A., and S.Ō. wrote the paper.

The authors declare no conflict of interest.

§To whom correspondence should be addressed. E-mail: omura@insti.kitasato-u.ac.jp.

This article contains supporting information online at www.pnas.org/cgi/content/full/0805504105/DCSupplemental.

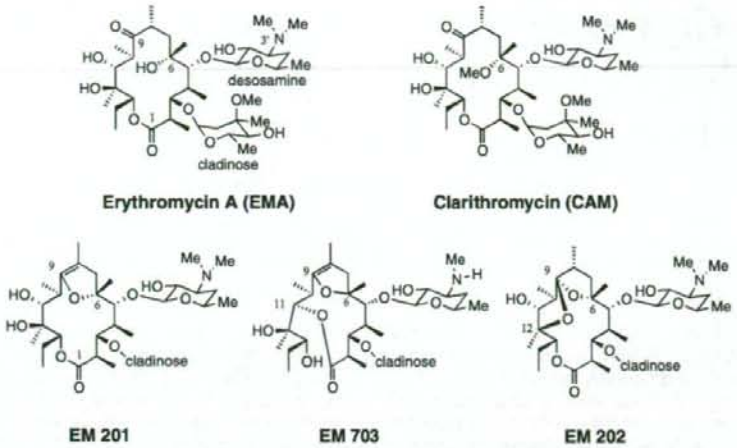

Fig. 1. Structure of EM derivatives.

Results

Effects of EM Derivatives on Viral Replication and Multinucleated Giant Cell Formation in M-Tropic HIV-1-Infected M-MΦs. We first examined whether EM derivatives (Fig. 1) have an ability to inhibit M-tropic HIV-1 replication in macrophage colony-stimulating factor (M-CSF)-induced monocyte-derived MΦs (M-MΦs), which express a high level of Hck and a large isoform of C/EBPβ, are susceptible to M-tropic HIV-1 replication, and whether they form multinucleated giant cells (MGC) by cell-to-cell fusion at 4–7 d after infection (10, 27). EM201 and EM703 (30 μM) completely inhibited viral replication and MGC formation at 7 d after infection, while EMA, CAM, and EM202 did not (Fig. 2*A*). PCR using a primer pair designed from the HIV-1 LTR region of HIV-1_{BaL} DNA at 2 d after infection showed that the DNA replication at first replicon was observed at similar levels in all of the M-MΦs. At 7 d after infection, however, the levels of viral DNA in M-MΦs treated with EMA, EM202, or DMSO (solvent) alone increased, whereas those in M-MΦs treated with EM201and EM703 remained low, at levels similar to those observed at 2 d after infection (Fig. 2*A*).

EM201 and EM703 (30 μM) persistently inhibited viral replication at 14 d (Fig. 2*B*), and inhibition was observed even at 21 d after infection (data not shown). EM201 and EM703 strongly inhibited HIV-1_{BaL} replication, even at 3 μM, and p24 levels were ~4% of those in cells treated with DMSO alone at 14 d after infection (Fig. 2*C*). EMA and EM202 induced inhibition of viral replication at higher concentration (>300 μM). However, the reduction curves in cells were similar to those in DMSO-treated cells (Fig. 2*C*), indicating the effects are mainly because of DMSO toxicity. In contrast, CAM partially but significantly inhibited HIV-1_{Bal} replication at 10–30 μM at 10 and 14 d after infection (Figs. 2 *B* and *C*), and it is impossible to deny that CAM itself can inhibit HIV-1 replication.

EM201 and EM703 Modulate the Expression of Hck and C/EBPβ Proteins in HIV-1_{BaL} Infected M-MΦs. To examine the possibility that EM201 and EM703 inhibit HIV-1 replication in M-MΦs via modulation of the expression of Hck and C/EBPβ, expression of these proteins in HIV-1 infected M-MΦs treated with 30 μM EM derivatives was examined by immunoblots at 2 d after infection. The levels of Hck protein in M-MΦs treated with EM201 and EM703 strongly decreased to one-seventh and one-ninth of that in M-MΦs treated with DMSO alone, respectively (Fig. 3*A*). Conversely, the small isoform of C/EBPβ protein was strongly induced in M-MΦs treated with EM201 and EM703, the levels increasing to 25- to 40-fold of that in M-MΦs treated with DMSO alone, with the L/S ratio of C/EBPβ markedly decreasing from 12.6 to 0.3 and 0.5, respectively (Fig. 3*A*).

EMA and EM202 did not affect the expression of Hck and C/EBPβ and consequently did not inhibit viral replication (Fig. 3*A*). Similarly CAM, which did not show inhibitory activity during the early phase of infection, did not significantly affect expression of either Hck or C/EBPβ at 2 d after infection.

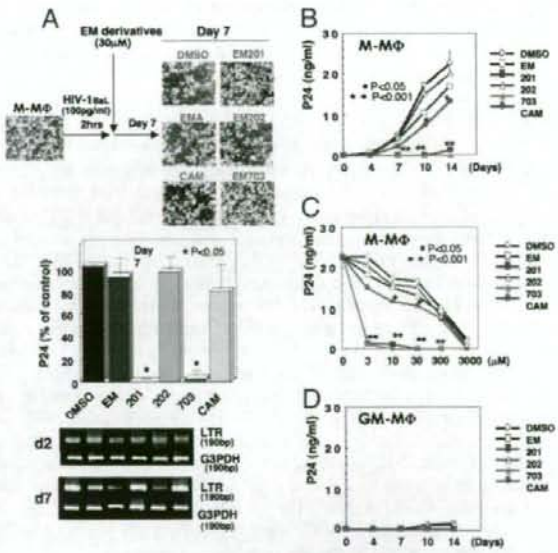

Fig. 2. Screening of EM derivatives that show an inhibitory effect on HIV-1_{BaL} replication in M-MΦs. (*A*) Effects of 30 μM of EMA (EM), CAM, EM201 (201), EM202 (202), and EM703 (703) on viral replication and MGC formation (Magnification, ×100) at 7 d after infection. The data of viral production were shown as the percentage of p24 antigen in control (DMSO alone) M-MΦs. The levels of viral DNA were assayed at 2 and 7 d after infection. (*B*) Kinetics of viral production in HIV-1 infected M-MΦs treated with 30 μM of EM derivatives. (*C*) Dose-response effects of EM derivatives on HIV-1 replication in M-MΦs at 14 d after infection. (*D*) EM derivatives (30 μM) do not change the resistant phenotype against HIV-1 infection in GM-MΦs. The data shown are representative one of five independent experiments.

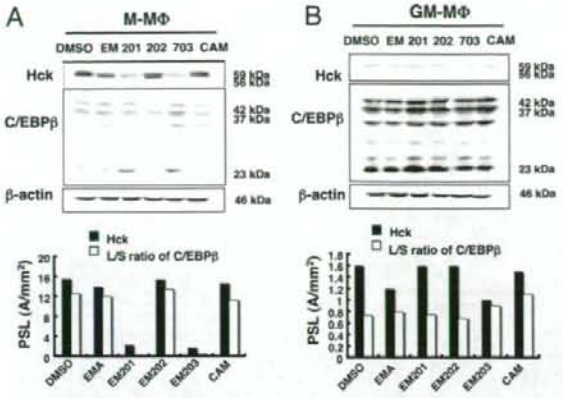

Fig. 3. Effects of EM derivatives on the expression of Hck and C/EBPβ in HIV-1_{BaL}-infected M-MΦs and GM-MΦs. Immunoblots of Hck and C/EBPβ in M-MΦs (*A*) and GM-MΦs (*B*) at 2 d after infection. EMA (EM), EM201 (201), EM202 (202), EM703 (703), and CAM were added at 30 μM. The relative amounts of Hck and C/EBPβ were measured using National Institutes of Health image software (PSL; photo stimulating luminescence, A/mm²). The relative amounts of the large band to the small band (L/S ratio) of C/EBPβ were calculated using PSL values of 37 kDa and 23 kDa of C/EBPβ isoforms and are shown at the bottom of each figure. The data shown are representative of one of three independent experiments.

EM201 and EM703 Change Neither the Expression of Hck and C/EBPβ Proteins Nor the Resistant Phenotype Against HIV-1 Infection in GM-MΦs. Granulocyte-macrophage CSF (GM-CSF)-induced monocyte-derived MΦ (GM-MΦ) is HIV-1 resistant and does not stimulate the replication of M-tropic HIV-1and MGC formation. This is because GM-MΦs express a high level of short isoforms of C/EBPβ and a low level of Hck, and HIV-1 infection drastically increases the expression of a short isoform of C/EBPβ but decreases that of Hck (10). We examined the effects of EM derivatives on viral replication and the expression of Hck and C/EBPβ in HIV-1_{BaL}-infected GM-MΦs. Even at 14 d after infection, we found that GM-MΦs treated with various kinds of EM derivatives (including EM201 and EM703) did not stimulate viral replication (Fig. 2*D*) or MGC formation (data not shown). Consistent with the lack of change in HIV-1 resistant phenotype, all of the EM derivatives did not affect the expression of Hck and C/EBPβ protein in GM-MΦs (Fig. 3*B*).

p38MAPK Inhibitor, but Not ERK1/2 Inhibitor, Inhibits Viral Replication in M-Tropic HIV-1 Infected M-MΦs via Reduced Expression of Hck and Increased Expression of a Small Isoform of C/EBPβ. Previous reports have shown that the replication of M-tropic HIV-1 in tissue MΦs requires the activation of p38MAPK (28) and that ERK1/2 mediates the activation of C/EBPβ (29, 30). We consequently examined the activation of MAPKs in HIV-1 susceptible M-MΦs and HIV-1 resistant GM-MΦs. Expressions of total and phosphorylated forms of p38MAPK in M-MΦs were higher than those in GM-MΦs before HIV-1_{BaL} infection (Fig. 4*A*). After infection, the phosphorylated form was augmented in M-MΦs but not in GM-MΦs (Fig. 4*A*). In contrast to p38MAPK, the expressions of total and phosphorylated forms of ERK1/2 in M-MΦs were lower than those in GM-MΦs before infection, but the expression was unchanged in both MΦs after infection (Fig. 4*A*). Consistent with the augumented activation of p38MAPK in M-MΦs, addition of p38MAPK inhibitor SB203580 (at 10 μM) completely suppressed viral replication and MGC formation in HIV-1_{BaL}-infected M-MΦs (Fig. 4*B*).

We subsequently investigated whether the inhibitory activity of SB203580 on viral replication in HIV-1_{BaL}-infected M-MΦs is mediated through modulation of the expression of Hck and C/EBPβ protein. SB203580 not only inhibited the phosphorylation of p38MAPK but also reduced the expression of Hck and increased the expression of the small isoform of C/EBPβ to mimic the inhibitory effect on viral replication (Fig. 4 *C–E*). Conversely, the ERK1/2 inhibitor PD98059 affected neither viral replication nor the expression of Hck and C/EBPβ protein (Fig. 4 *B–E*).

EM201 and EM703 Inhibit Viral Replication in M-Tropic HIV-1 Infected M-MΦs via Inhibition of p38MAPK Activation. The above results suggest that EM201 and EM703 inhibit M-tropic HIV-1 replication

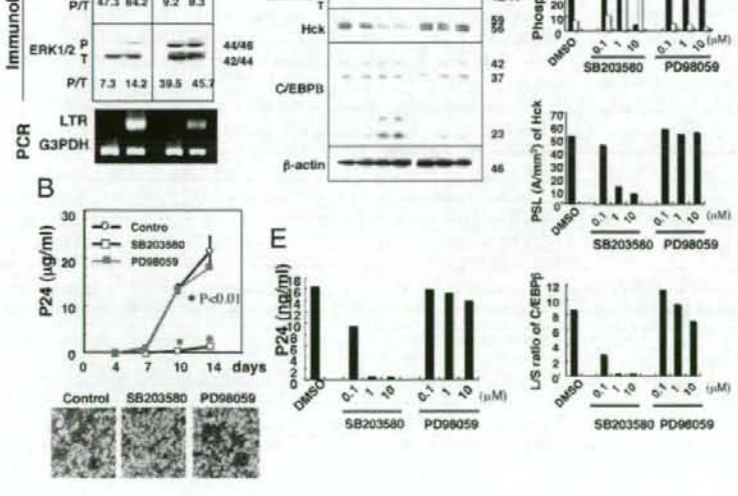

Fig. 4. Effects of p38 MAPK inhibitor and ERK1/2 inhibitor on viral replication and expression of Hck and C/EBPβ in HIV-1_{BaL}infected M-MΦs. (*A*) Immunoblot analysis of total and phosphorylated forms of p38MAPK and ERK1/2 in M-MΦs and GM-MΦs before and 2 d after infection. (*B*) Kinetic analysis of viral replication and morphology in HIV-1_{BaL}-infected M-MΦs treated with 10 μM of SB203580 or PD98059. (*C*) Immunoblot analysis of Hck and C/EBPβ in HIV-1_{BaL}-infected M-MΦs treated with various concentrations of SB203580 or PD98059 at 2 d after infection. (*D*) The relative amounts of Hck and L/S ratio of C/EBPβ in the cells or the phosphorylated protein *P* to the total protein *T* (P/T ratio) of p38 MAPK and ERK1/2 in immunoblot analysis shown in c calculated as described in Fig. 3. (*E*) Viral production in HIV-1_{BaL}-infected M-MΦs treated with various concentrations of SB203580 or PD98059. The data shown are representative of one of three independent experiments.

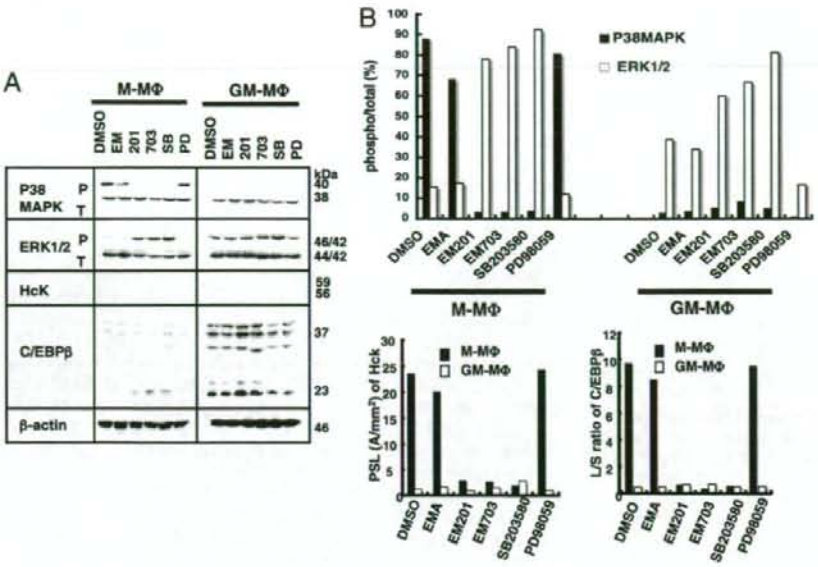

Fig. 5. Effects of EM derivatives on the phosphorylation of p38 MAPK and ERK1/2 in M-MΦs and GM-MΦs. (*A*) Immunoblot analysis of Hck and C/EBPβ, and the phosphorylation of p38 MAPK and ERK1/2 in M-MΦs and GM-MΦs treated with 30 μM of EMA (EM), EM201 (201), EM703 (703), 10 μM of SB203580 (SB), or PD98059 (PD), and DMSO alone at 2 d after HIV-1 infection. (*B*) The relative amounts of Hck and L/S ratio of C/EBPβ or P/T ratio of p38 MAPK and ERK1/2 in immunoblot analysis shown in a are calculated as described in Fig. 3. The data shown are representative of one of three independent experiments.

via inhibition of p38MAPK activation. To help confirm this hypothesis, we examined the effect of EM201 or EM703 (30 μM) on the phosphorylation of p38MAPK and ERK1/2 in M-MΦs by immunoblot. EM201 and EM703, but not EMA, reduced phosphorylation of p38MAPK but enhanced the phosphorylation of ERK1/2 in HIV-1-infected M-MΦs at 2 d after treatment (Fig. 5).

As described above, EM201 and EM703 did not affect the HIV-1-resistant phenotype of GM-MΦs (Figs. 2*D* and 3*B*). Consistent with the results, none of the EM derivatives significantly affected the phosphorylation pattern of p38MAPK and ERK1/2 in HIV-1-infected GM-MΦs (Fig. 5).

Activated CD4⁺T Cells Stimulate Viral Replication in M-Tropic HIV-1 Infected GM-MΦs via Down-Regulation of a Small Isoform of C/EBPβ. Recently, Hosino *et al.* (9) reported a phenotypical change of human alveolar MΦs (A-MΦs) from resistant to susceptible for HIV-1 replication caused by the addition of activated lymphocytes. The change was brought about by decreased expression of a small isoform of C/EBPβ (9). In line with this report, the addition of activated CD4⁺T cells to HIV-1_{BaL}-infected GM-MΦs stimulated marked viral replication (Fig. 6*A*), with MGC formation and clusters of GM-MΦs with CD4⁺ T cells (data not shown) at 10–14 d after infection. The amounts of viral DNA in the GM-MΦs increased at 2–7 d after infection (Fig. 6*B*). In GM-MΦs stimulated with activated CD4⁺ T cells, expression of the small isoform of C/EBPβ protein significantly decreased whereas the L/S ratio of C/EBPβ increased (from 0.57 to 3.6) at 2 d after infection (Fig. 6 *C* and *D*). Expression of Hck in the GM-MΦs, however, did not change significantly, even after stimulation with activated T cells and was very low compared with that in M-MΦs (Fig. 6 *C* and *D*).

Activated CD4⁺T Cells Down-Regulate the Small Isoform of C/EBPβ in M-Tropic HIV-1-Infected GM-MΦs via Augmentation of ERK1/2 Phosphorylation. As described above, activation of p38MAPK but not ERK1/2 is critical for HIV-1 replication in M-MΦs. However, the p38MAPK inhibitor, SB203580, did not inhibit viral replication in GM-MΦs stimulated with activated CD4⁺T cells (Fig. 6*A*). Instead, the ERK1/2 inhibitor PD98059 completely inhibited viral replication (Fig. 6*A*) and suppressed the level of viral DNA to that observed in the culture of GM-MΦs alone in which viral replication was absent (Fig. 6*B*). Upon examination of the phosphorylation of p38MAPK and ERK1/2 in HIV-1_{BaL}-infected GM-MΦs stimulated with activated CD4⁺ T cells, the phosphorylation ratio of ERK1/2 but not of p38MAPK significantly increased in GM-MΦs stimulated with activated CD4⁺ T cells, compared with that in GM-MΦs alone. Addition of PD98059 not only inhibited the phosphorylation of ERK1/2 but also increased expression of the small isoform of C/EBPβ, while markedly decreasing the L/S ratio of C/EBPβ from 3.6 to 0.82 (Fig. 6 *C* and *D*). The addition of SB203580 did not affect the expression of C/EBPβ. The expression of Hck was unaffected by treatment with either of the two inhibitors (Fig. 6 *C* and *D*).

EM201 and EM703 Inhibit M-Tropic HIV-1 Replication in GM-MΦs Stimulated with Activated CD4⁺ T Cells via Inhibition of the Activation of ERK1/2 and Augmentation of the Expression of the Small Isoform of C/EBPβ. In examining whether EM201 and EM703 can inhibit viral replication in M-tropic HIV-1-infected GM-MΦs stimulated with activated CD4⁺T cells, addition of EM201 and EM703 (30 μM) completely inhibited viral replication (Fig. 6*A*) and MGC formation (data not shown). The levels of HIV-1 DNA observed were very low, the same as those seen in the culture of GM-MΦs alone (Fig. 6*B*).

We subsequently examined the effects of EM201 and EM703 on the expression of Hck and C/EBPβ and on the phosphorylation of p38MAPK and ERK1/2 in HIV-1_{BaL}-infected GM-MΦs stimulated with activated CD4⁺ T cells at 2 d after infection by immunoblot. Treatment with EM201 and EM703 did not change the levels of Hck protein, but increased levels of the small isoform of C/EBPβ protein and the L/S ratio of C/EBPβ decreased from 3.6 to 0.45 (EM201) and 0.44 (EM703) (Fig. 6 *C* and *D*). The phosphorylation level of ERK1/2 decreased following treatment with EM201 and EM703, but that of p38MAPK remained unchanged (Fig. 6 *C* and *E*).

Discussion

In this study, we demonstrated that two EMA derivatives, EM201and EM703, can inhibit the replication of M-tropic HIV-1 in tissue MΦs at the posttranscriptional and translational levels, but do not affect viral entry and first DNA replicon. The inhibition is

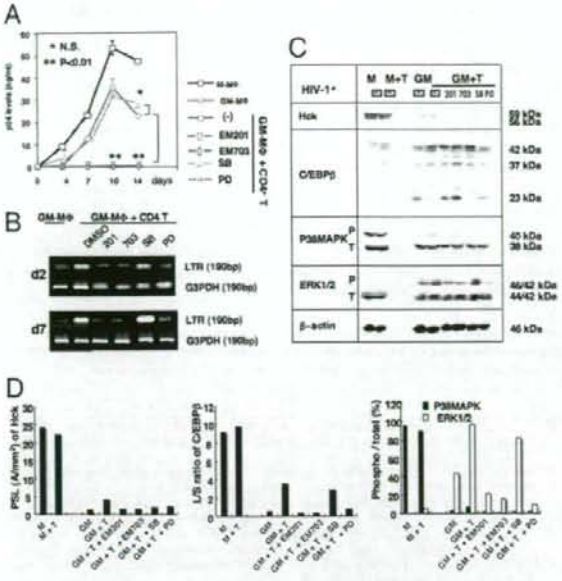

Fig. 6. Augmentation of M-tropic HIV-1 production in GM-MΦs stimulated with CD4$^+$ T cells, and the suppressive effects of EM201 and EM703 on viral replication through the induction of small isoforms of C/EBPβ via inhibition of phosphorylation of ERK1/2. M-MΦs and GM-MΦs were infected with HIV-1_{Ba-L}. Part of HIV-1-infected GM-MΦs were stimulated with activated CD4$^+$ T cells and incubated with or without 30 μM of EMA (EM), EM201 (201), or EM703 (703), 10 μM of SB203580 (SB), or PD98059 (PD), and DMSO alone. (*A*) Kinetic analysis of HIV-1 replication. (*B*) Levels of viral DNA at 2 and 7 d after infection. (*C*) Immunoblot analysis of Hck, C/EBPβ, and phosphorylation of p38 MAPK and ERK1/2 at 2 d after infection. (*D*) The relative amounts of Hck and L/S ratio of C/EBPβ or P/T ratio of p38 MAPK and ERK1/2 in immunoblot analysis shown in *c* calculated as described in Fig. 3. (*M*) M-MΦ; GM, GM-MΦ; T, T cells; 201, EM201; 703, EM703; SB, SB203580; and PD, PD98059. The data shown are representative of one of three independent experiments.

caused by a new means of converting the phenotype of tissue MΦs, from HIV-1 susceptible to HIV-1 resistant, via down-regulation of Hck and induction of the small isoform of C/EBPβ through modulation of the activation of MAPKs. Consistent with the previous report (9), we showed that HIV-1-resistant GM-MΦs, require stimulation with activated CD4$^+$T cells to produce vigorous virus production. This is mediated by down-regulation of the expression of the small isoform of C/EBPβ. Both EM201 and EM703 potently inhibit viral replication, not only in M-MΦs but also in GM-MΦs stimulated with activated CD4$^+$T cells via inhibiting the down-regulation of the expression of the small isoform of C/EBPβ.

Both EM201 and EM703 change the phenotype only of HIV-1-susceptible MΦs. They do not affect the phenotype of HIV-1-resistant GM-MΦs. HIV-1 susceptibility and the expression of Hck and C/EBPβ proteins in A-MΦs from normal healthy volunteers are the same as those in GM-MΦs (8, 10). Therefore EM201 and EM703 do not change the resistant phenotype of A-MΦs. This would be beneficial for healthy A-MΦs in the HIV-1 carrier, by maintaining resistance against HIV-1 replication.

In the present study, we demonstrated that activation of p38MAPK and ERK1/2 play a critical role in HIV-1 production via down-regulation of the small isoform of C/EBPβ in HIV-1-infected-M-MΦs and -GM-MΦs stimulated with activated CD4$^+$T cells, respectively. This study shows that different MAPKs play crucial roles in HIV-1 production in different types of tissue MΦs. P38MAPK activation in HIV-1-infected M-MΦs link to the augmented expression of Hck and the maintenance of the low level of the small isoform of C/EBPβ. We previously reported that reduced expression of Hck in M-MΦs with antisense oligonucleotide for Hck stimulates the induction of the short isoform of C/EBPβ and inhibits the viral replication (10). Our present results, taken together with the previous study, show the unique evidence that the p38MAPK signal cascade is upstream of Hck expression and is linked to down-regulation of the small isoform of C/EBPβ in HIV-1-susceptible M-MΦs. However, ERK1/2-mediated down-regulation of the small isoform of C/EBPβ in HIV-1-infected GM-MΦs stimulated with activated CD4$^+$T cells does not link to Hck expression.

Interestingly, EM201 and EM703, in contrast to existing MAPK inhibitors, can inhibit viral replication via prevention of the activation of respective MAPKs in both HIV-1-infected-M-MΦs and -GM-MΦs stimulated with activated T cells, where different MAPKs play a critical role for viral replication. Such a novel and unique suppressive mechanism of EM201 and EM703 on HIV-1 replication in tissue MΦs may be useful for the future treatment of AIDS patient.

The anti-HIV-1 activity of EM201 and EM703 does not relate to their antibiotic activity, because they have only weak (EM201) or completely lack (EM703) such antibiotic activity (24, 25). At present, we do not know what kind of structure activity relationships exist in EM201 and EM703. Recently, calmodulin- and calmodulin-dependent protein kinase-II (CaMK-II)-dependent activation of p38MAPK has been reported in HIV accessory protein, Tat-induced IL-10 expression in normal human monocytes (31). EM201 and EM703 are known to act as inhibitors of intracellular Ca^{2+} level and Ca^{2+} oscillation (21, 32, 33). These characteristics may contribute to the novel anti-HIV-1 mechanism of EM201 and EM703.

Macrolides, such as EMA and CAM, are known to be specifically accumulated into tissue MΦs and stay stable at high levels for long periods because of a low rate of breakdown and excretion (34). EM201 and EM703 potently inhibit HIV-1 replication in MΦs at low levels, such as 30 μM, that correspond to the concentration of EMA or CAM in MΦs after oral intake of EMA, 400 mg or CAM 200 mg/day (usual doses are 1600 mg and 400 mg/day, respectively). Furthermore, inhibition of viral replication can be observed at lower concentrations, such as 3 μM, which is sustained for 2–14 days after infection. These findings offer advantages with respect to drug specificity and reduction of drug toxicity. In addition, these new macrolides are derived from EMA (24, 25) and would be very inexpensive. Thus, these substances offer great potential for the creation of new anti-HIV-1 drugs for the future treatment of AIDS patients.

Materials and Methods

Erythromycin Derivatives. EMA was purchased from Sigma-Aldrich. CAM was supplied by Taisho Pharmaceutical. EM201, EM202, and EM703 were prepared as described previously (24, 25).

Preparation and Culture of MΦs. Monocytes (Mos) and Mo-derived Mp were prepared as described previously (10, 35). M-CSF-induced monocyte-derived MΦs and GM-CSF-induced monocyte-derived MΦs were called M-MΦs and GM-MΦs, respectively. [see supporting information (SI) *Materials and Methods* for a detailed description].

HIV-1 Strain and Infection. M-tropic HIV-1 strain, HIV-1_{Ba-L}, was collected from culture supernatant of the HIV-1 strain-infected M-MΦs as a viral resource. Mo-derived MΦs were incubated for 2 h at 37°C with 100 pg/ml p24 antigen of DNase-treated viral supernatant (p24, the 50% tissue culture infective dose ($TCID_{50}$) and multiplicity of infection (MOI) are 50 ng/ml, ~3,000 and 0.05, respectively) and then cultured in RPMI MEDIUM 1640 containing 10% FCS and CSF. If necessary, the viral inoculum was pretreated with 100 μM AZT for 2 h at 4°C (5). Fresh culture medium containing CSF was added every 3–4 d (20% of the volume). Heat-inactivated virus (1 h, 56°C) was used as negative control. Viral production was assayed by sequential measurement of p24 antigen in superna-

MICROBIOLOGY

tants by an ELISA using a combination of two antibodies; anti-*gag*-p24 monoclonal antibody (Nu24) and peroxidase-labeled 10B5 (36), or the RETRO-TEK HIV-1 p24 antigen ELISA kit for high-affinity detection of low levels of p24 antigen (ZeptoMetrix, Buffalo, New York).

Coculture of HIV-1 Infected GM-MΦs with the Activated CD4⁺T Cells. $CD4^+$ T cells were positively isolated from $CD14^-$ PBMCs using a MACS with anti-CD4 mAb coated microbeads. The selected population was >93% positive for CD3 and CD4. Activated $CD4^+$ T cells were prepared by stimulation with PHA and cultured with IL-2 (30 unit/ml) (Genzyme). GM-MΦs were incubated for 2 h at 37°C with 100 pg/ml p24 antigen of DNase-treated viral supernatant, washed twice, and then cocultured with the activated $CD4^+$ T cells in the presence of IL-2.

Detection of HIV-1 DNA by Nested PCR. Detection of HIV-1 DNA by nested PCR was performed as described previoiusly (10). HIV LTR and *gag* primers were JAM 62 and JAM 65. For the nested PCR, JAM 63 and JAM 64 were used as internal primers (36). (see *SI Materials and Methods* for a detailed description).

Immunblot Analysis. Immunoblot analysis was performed as described in ref. 10. Antibodies against the following proteins were used: rabbit polyclonal antibody against Hck (N-30), C/EBPβ (C-19) (Santa Cruz Biotechnology), phospho-specific (Tyr 182) p38 mitogen-activated protein kinase (P38MAPK) (no. 9211), p38 MAPK (no. 9212), phospho-specific (Tyr 204) phosphorylated extracellular signal-regulated kinases (ERK)1/2 (no. 9101), ERK1/2 antibody (no. 9102) (New England BioLabs), or normal rabbit IgG. Horseradish peroxidase-conjugated goat anti-rabbit IfG (sx-2030)(Santa Cruz Biotechnology) was used as secondary Ab. The blots were visualized with Amersham ECL Reagent on Hyper ECL-film (Amersham). (see *SI Materials and Methods* for a detailed description).

Statistical Analysis. Statistical analysis of the data were performed using Student's *t test*. *P*-values <0.01 were considered significant. The experiments shown are representatives of three to seven independent experiments.

ACKNOWLEDGMENTS. This work was supported in part by grants for Research on Health Sciences Focusing on Drug Innovation from the Japan Health Sciences Foundation and the Ministry of Health, Labor and Welfare of Japan.

1. Cavert W, *et al.* (1997) Kinetics of response in lymphoid tissues to antiretroviral therapy of HIV-1 infection. *Science* 276:960–964.
2. Perelson AS, *et al.* (1997) Decay characteristics of HIV-1-infected compartments during combination therapy. *Nature* 387:188–191.
3. Orenstein JM, Fox C, Wahl SM (1997) Macrophages as a source of HIV during opportunistic infections. *Science* 276:1857–1861.
4. Crowe SM, Sonza S (2000) HIV-1 can be recovered from a variety of cells including peripheral blood monocytes of patients receiving highly active antiretroviral therapy: A further obstacle to eradication. *J Leukoc Biol* 68:345–350.
5. Orenstein JM (2001) The macrophage in HIV infection. *Immunobiol* 204:598–602.
6. Nakata K, *et al.* (1997) Mycobacterium tuberculosis enhances human immunodeficiency virus-1 replication in the lung. *Am J Resp Crit Care Med* 155:996–1003.
7. Whalen C, *et al.* (1995) Accelerated course of human immunodeficiency virus infection after tuberculosis. *Am J Respir Crit Care Med* 151:129–135.
8. Honda Y, *et al.* (1998) Type I interferon induces inhibitory 16-kD CCAAT/enhancer binding protein (C/EBP)beta, repressing the HIV-1 long terminal repeat in macrophages: Pulmonary tuberculosis alters C/EBP expression, enhancing HIV-1 replication. *J Exp Med* 188:1255–1265.
9. Hoshino Y, *et al.* (2002) Maximal HIV-1 replication in alveolar macrophages during tuberculosis requires both lymphocyte contact and cytokines. *J Exp Med* 195:495–505.
10. Komuro I, Yokota Y, Yasuda S, Iwamoto A, Akagawa KS (2003) CSF-induced and HIV-1-mediated distinct regulation of Hck and C/EBPbeta represent a heterogeneous susceptibility of monocyte-derived macrophages to M-tropic HIV-1 infection. *J Exp Med* 198:443–453.
11. Henderson AJ, Calame KL (1997) CCAAT/enhancer binding protein (C/EBP) sites are required for HIV-1 replication in primary macrophages but not CD4(+) T cells. *Proc Natl Acad Sci USA* 94:8714–8719.
12. Weiden M, *et al.* (2000) Differentiation of monocytes to macrophages switches the mycobacterium tuberculosis effect on HIV-1 replication from stimulation to inhibition: Modulation of interferon response and CCAAT/enhancer binding protein beta expression Type I interferon induces inhibitory 16-kD CCAAT/enhancer binding protein (C/EBP)beta, repressing the HIV-1 long terminal repeat in macrophages: Pulmonary tuberculosis alters C/EBP expression, enhancing HIV-1 replication. *J Immunol* 165:2028–2039.
13. Hogan TH, Krebs FC, Wigdahl B (2002) Regulation of human immunodeficiency virus type 1 gene expression and pathogenesis by CCAAT/enhancer binding proteins in cells of the monocyte/macrophage lineage. *J Neurovirol* 8 Suppl 2:21–26.
14. Kudoh S, Uetake K, Hagiwara K (1987) Clinical effect of low dose long term erythromycin chemotherapy on diffuse panbronchiolitis. *Jap J Thorac Dis* 25:632–642.
15. Kadota J, *et al.* (1993) A mechanism of erythromycin treatment in patients with diffuse panbronchiolitis. *Am Rev Respir Dis* 147:153–159.
16. Sugawara E (1997) Effect of macrolide antibiotics on neutrophil function in human peripheral blood. *Kansenshogaku Zasshi* 71:329–336.
17. Sunazuka T, *et al.* (1999) Effects of erythromycin and its derivatives on Interleukin-8 release by human bronchial epithelial cell line BEAS-2B cells. *J Antibiot* 52:71–74.
18. Oohori M, *et al.* (2000) Effect of 14-membered ring macrolide compounds on rat leucocytes chemotaxis and the structure-activity relationships. *J Antibiot* 53:1219–1222.
19. Keicho N, Kudoh S, Yotsumoto H, Akagawa KS (1993) Erythromycin promotes monocytes to macrophage differentiation. *J Antibiot* 47:80–89.
20. Keicho N, Kudoh S, Yotsumoto H, Akagawa KS (1993) Antilymphocytic activity of erythromycin distinct from that of FK506 or cyclosporin A. *J Antibiot* 46:1406–1413.
21. Kudoh S, *et al.* (2002) Novel activity of erythromycin and its derivatives. *Macrolide Antibiotics, Chemistry, Biology, and Practice*, eds Omura S (Academic), 2nd Ed, pp 533–569.
22. Culic O, Erakovic V, Parnham MJ (2001) Anti-inflammatory effects of macrolide antibiotics. *Eur J Pharmacol* 429:209–229.
23. Labro MT (2001) Anti-inflammatory activity of macrolides: A new therapeutic potential? *J Antimicrob Chemother* 41(Suppl B):37–46.
24. Sunazuka T, *et al.* (2003) Effect of 14-membered macrolide compounds on monocyte to macrophage differentiation. *J Antibiot* 5:721–724.
25. Yoshida K, *et al.* (2005) Macrolides with promotive activity of monocyte to macrophage differentiation. *J Antibiot* 58:79–81.
26. Ying JL, *et al.* (2006) EM703 improves bleomycin-induced pulmonary fibrosis in mice by the inhibition of TGF-beta signaling in lung fibroblasts. *Respir Res* 7:16:1–13.
27. Matsuda S, *et al.* (1995) Suppression of HIV replication in human monocyte-derived macrophages induced by granulocyte/macrophage colony-stimulating factor. *AIDS Res Hum Retroviruses* 11:1031–1038.
28. Muthumani K, *et al.* (2004) Suppression of HIV-1 viral replication and cellular pathogenesis by a novel p38/JNK kinase inhibitor. *Aids* 18:739–748.
29. Nakajima T, *et al.* (1993) Phosphorylation at threonine-235 by a ras-dependent mitogen-activated protein kinase cascade is essential for transcription factor NF-IL6. *Proc Natl Acad Sci USA* 90:2207–2211.
30. Giltiay NV, Karakashian AA, Alimov AP, Ligthle S, Nikolova-Karakashian MN (2005) Ceramide- and ERK-dependent pathway for the activation of CCAAT/enhancer binding protein by interleukin-1beta in hepatocytes. *J Lipid Res* 46:2497–2505.
31. Gee K, Angel JB, Mishra S, Blahoianu MA, Kumar A (2007) IL-10 regulation by HIV-Tat in primary human monocytic cells: Involvement of calmodulin/calmodulin-dependent protein kinase-activated p38 MAPK and Sp-1 and CREB-1 transcription factors. *J Immunol* 178:798–807.
32. Sunazuka T, Omura S (2004) Creation of a new macrolide derivative, EM703. *Jpn J Antibiot* 57(Suppl A):114–116.
33. Hattori R, Shimizu T, Shimizu S, Majima Y (2004) Effect of EM703, a new macrolide derivative, on mucus secretion from the airway epithelial cells. *Jpn J Antibiot* 57(Suppl A):123–125.
34. Fietta A, Merlini C, Gialdroni GG (1997) Requirements for intracellular accumulation and release of clarithromycin and azithromycin by human phagocytes. *J chemotherapy* 9:23–31.
35. Akagawa KS (2002) Functional heterogeneity of colony-stimulating factor induced human monocyte-derived macrophages. *Int J Hematol* 76:27–34.
36. Tsunetsugu-Yokota Y, *et al.* (1995) Monocyte-derived cultured dendritic cells are susceptible to human immunodeficiency virus infection and transmit virus to resting T cells in the process of nominal antigen presentation. *J Virol* 69:4544–4547.

Biochemical and Biophysical Research Communications 377 (2008) 7–11

Contents lists available at ScienceDirect

Biochemical and Biophysical Research Communications

journal homepage: www.elsevier.com/locate/ybbrc

A recombinant replication-competent hepatitis C virus expressing Azami-Green, a bright green-emitting fluorescent protein, suitable for visualization of infected cells

Wei Hou [a], Chie Aoki [a,b], Lijuan Yu [a], Xianzi Wen [a], Yinhuan Xue [a], Bin Gao [a], Wenjun Liu [a], George Fu Gao [a], Aikichi Iwamoto [a,b,c], Yoshihiro Kitamura [a,b,*]

[a] China–Japan Joint Laboratory of Molecular Immunology and Molecular Microbiology, Institute of Microbiology, Chinese Academy of Sciences, No. A 3 Datun Road, Chaoyang District, Beijing 100101, China
[b] Research Center for Asian Infectious Diseases, The Institute of Medical Science, The University of Tokyo, 4-6-1 Shirokanedai, Minato-ku, Tokyo 108-8639, Japan
[c] Division of Infectious Diseases, Advanced Clinical Research Center, The Institute of Medical Science, The University of Tokyo, 4-6-1 Shirokanedai, Minato-ku, Tokyo 108-8639, Japan

ARTICLE INFO

Article history:
Received 30 July 2008
Available online 9 September 2008

Keywords:
Hepatitis C virus
JFH1
Azami-Green
Nonstructural protein 5A
Interferon

ABSTRACT

The hepatitis C virus (HCV) production system consists of transfecting the human hepatoma cell line Huh7 with genomic HCV RNA (JFH1). To monitor HCV replication by fluorescence microscopy, we constructed a recombinant HCV clone expressing Azami-Green (mAG), a bright green fluorescent protein, by inserting the mAG gene into the nonstructural protein 5A (NS5A) gene; the resultant clone was designated JFH1-hmAG. The Huh-7.5.1 (a subclone of Huh7) cells transfected with JFH1-hmAG RNA were found to produce cytoplasmic NS5A-mAG, as readily visualized by fluorescence microscopy, and infectious virus, as assayed with the culture supernatant, indicating that JFH1-hmAG is infectious and replication-competent. Furthermore, the replication of this virus was inhibited by interferon alpha in a dose-dependent manner. These results suggest that JFH1-hmAG is useful for studying HCV life cycle and the mechanism of interferon's anti-HCV action and for screening and testing new anti-HCV drugs.

Hepatitis C virus (HCV), a positive-strand RNA virus, which belongs to *Flaviviridae*, causes serious chronic hepatitis that results in cirrhosis and hepatocellular carcinoma. Recently, cell culture systems supporting HCV replication have been developed with the complementary DNA clones of the genotype 2a isolate JFH1 [1–7] and the genotype 1a isolate H77S [8]. These systems have been shown to greatly contribute to the studies of HCV biology and the development of novel antiviral strategies against HCV [9–24]. However, the procedures for quantitative analysis of HCV are considerably complicated, because the yield of HCV in cell cultures is fairly low. Moreover, observation of living infected cells has been impossible. For solving these problems, development of recombinant HCV carrying a reporter gene such as *Renilla* luciferase or red/green fluorescent protein gene has been attempted [25–27].

A green-emitting fluorescent protein, Azami-Green (AG, tetrameric) has been identified in a stony coral, *Azami-Sango* [28]. Its monomeric derivative (mAG) is stably brilliant independently of pH and thus suitable for labeling proteins or subcellular structures in mammalian cells [28]. Most importantly, as far as we know, mAG is the brightest among the monomeric forms of green-emitting fluorescent proteins; for example, it is approximately 1.23-fold brighter than EGFP from *Aequorea victoria* [28,29] (brightness is calculated as a product of molar extinction coefficient and fluorescence quantum yield). In this study, inserting an mAG gene with humanized codon usage (hmAG) into the nonstructural protein 5A (NS5A)-coding sequence, we generated a novel replication-competent HCV clone. The brightness of the mAG allowed us to visualize infected cells with high sensitivity and ease.

Materials and methods

HCV plasmid construction. The DNA fragment encoding a monomeric Azami-Green (mAG) with the *Xho*I sites (C'TCGAG) at both ends was obtained by PCR using phmAG1-MC1 (MBL, Tokyo, Japan) as a template, digested with *Xho*I, and inserted into the *Abs*I site (5′-CCTCGAGG-3′) of pJFH1 [1] (GenBank Accession No. AB047639). The integrity of the resulting plasmid, pJFH1-hmAG was verified by DNA sequencing (Fig. 1).

RNA synthesis. We followed previously developed methods [30]. In brief, we cut pJFH1-hmAG with *Xba*I and treated it with Mung

* Corresponding author. Address: China–Japan Joint Laboratory of Molecular Immunology and Molecular Microbiology, Institute of Microbiology, Chinese Academy of Sciences, No. A 3 Datun Road, Chaoyang District, Beijing 100101, China.
E-mail address: kitamura@im.ac.cn (Y. Kitamura).

0006-291X/$ - see front matter © 2008 Elsevier Inc. All rights reserved.
doi:10.1016/j.bbrc.2008.08.145

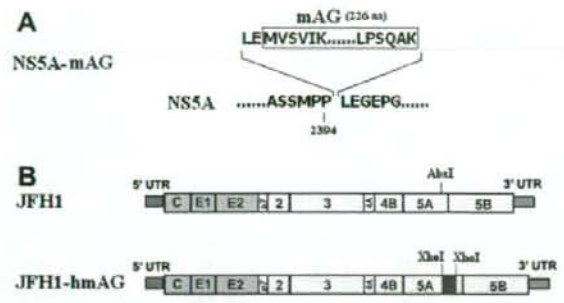

Fig. 1. HCV plasmids. (A) Sites and amino acid sequences of the mAG insertion in NS5A. (B) Schematic diagrams of JFH1 and its derivative JFH1-hmAG containing the hmAG gene within the NS5A gene.

Bean nuclease (New England Biolabs) to remove the 3′-protruding four nucleotides. With this DNA, we synthesized HCV RNA by using a MEGAscript™ T7 kit (Applied Biosystems/Ambion, TX). We treated the synthesized RNA with DNaseI (Promega, WI) at 37 °C for 15 min, and extracted it with acid phenol to remove remaining template DNA.

Cell cultures and transfection. Huh-7.5.1 cells [2], which are highly permissive to HCV RNA replication, were maintained in Dulbecco's modified Eagle's medium (DMEM) (Sigma-Aldrich, MO) supplemented with 10% fetal bovine serum (Invitrogen Corporation/Gibco, CA), 100 μg/mL of kanamycin (Sigma), and non-essential amino acids (Invitrogen Corporation/Gibco). The synthesized RNA of JFH1-hmAG was delivered to cells by electroporation or lipofection. We performed electroporation with a Gene Pulser II apparatus (Bio-Rad Laboratories, CA) as described [1], and lipofection with UniFECTOR reagent (B-Bridge International, Tokyo, Japan); a mixture of 6 μg of JFH1-hmAG RNA and 36 μl of UniFECTOR was subjected to 10^6 cells in a 100-mm culture dish.

Immunofluorescence analysis. Intracellular staining was performed as described [2]. In brief, a anti-Core mouse monoclonal antibody (IgG1, clone Hyb-K0811B, Cosmo Bio, Tokyo, Japan) was used at a dilution of 1:200 followed by incubation with a 1:400 dilution of Alexa Fluor 594-conjugated donkey anti-mouse antibody (Invitrogen Corporation/Molecular Probes, CA). Cell nuclei were stained with 4,6-diamidino-2-phenylindole (DAPI, Sigma-Aldrich). Images were acquired by using Biozero fluorescence microscopy (Keyence, Tokyo, Japan) or with a confocal microscope Leica TCS SP2 (Leica Microsystems GmbH, Wetzlar, Germany).

Infection. Huh-7.5.1 cells were seeded 24 h before infection at a density of 2×10^4 cells/well in a 8-well culture slide (BD BioCoat™, poly-D-lysine coated 8-well CultureSlide, BD, NJ). The cells were inoculated with the culture supernatant obtained from the cells transfected with JFH1-hmAG RNA for 3 h, washed three times with PBS, then cultured in 0.5 mL/well of the complete culture medium.

Reverse transcription (RT) PCR. RNA was extracted from cell culture supernatant with ISOGEN-LS (Nippon GENE, Tokyo, Japan) or from cells with ISOGEN (Nippon GENE). Complementary DNA was generated by a ReverTra Ace qPCR RT kit (Toyobo, Osaka, Japan) according to manufacturer's instructions. PCRs targeting the different regions along the JFH1-hmAG genome were performed. The primers for PCR were as follows: for the 5′-untranslated region (5′UTR), 5′-TCTGCGGAACCGGTGAGTAC-3′ and 5′-TCAGGCAGTACCACAAGGCC-3′); for the nonstructural protein 3 (NS3) region, 5′-CTTTGACTCCGTGATCGACC-3′ and 5′-CCCTGTCTTCCTCTACCTG-3′; and for the NS5A-hmAG junction, 5′-CTGGCCATCAAGACCTTTG-3′ and 5′-GCTTGAAGTAGTCCTGGATG-3′.

Interferon inhibition. Huh-7.5.1 cells were incubated for 12 h with various concentrations of interferon alpha (IFNα, Universal Type I Interferon, PBL InterferonSource, NJ), then incubated with the culture supernatant containing JFH1-hmAG virus for 3 h, washed twice with PBS, and further incubated for 3 days. The copy numbers of intracellular HCV RNA were determined by quantitative RT-PCR (RT-qPCR). RT-qPCR with a LightCycler 2.0 Instrument (Roche) allowed us to determine relative copy numbers by normalization with that of GAPDH mRNA. The primers for RT-qPCR were as follows: for HCV, 5′-TCTGCGGAACCGGTGAGTA-3′ (sense) and 5′-TCAGGCAGTACCACAAGGC-3′ (antisense); and for GAPDH, 5′-GAAGGTGAAGGTCGGAGTC-3′ (sense) and 5′-GAAGATGGTGATGGGATTTC-3′ (antisense), as described previously [2,31].

Results and discussion

Construction of pJFH1-hmAG and direct visualization of NS5A-mAG by fluorescent microscopy

We constructed a novel HCV clone (JFH1-hmAG) containing the hmAG sequence fused with NS5A at the amino acid 418 of NS5A (see Materials and methods for detail. Fig. 1). Three days after transfection of Huh-7.5.1 cells with JFH1-hmAG RNA, the green signal of the NS5A-mAG fluorescence was strong enough to be readily visualized in the cytoplasm as bright dots in a reticular pattern surrounding the nucleus by confocal microscopy (Fig. 2A). To further confirm viral protein production, we stained the cells with anti-Core antibody (Fig. 2B, upper right) and found the signal in a pattern similar to that of NS5A-mAG. Indeed, merging the NS5A-mAG and Core images (Fig. 2B, lower right), we observed partial colocalization of NS5A-mAG and Core, shown as yellow signals. Since the wild-type JFH1 has been reported to show the same colocalization pattern [25,32], JFH1-hmAG seems to inherit this property from the wild-type JFH1. Furthermore, RT-PCR with the RNA extracted from these transfected cells showed that the NS5A-hmAG junction in the JFH1-hmAG genome was stably retained (data not shown). Further studies seem necessary to determine the stability of NS5A-mAG over more extended passages indicator.

Inoculation of naïve Huh-7.5.1 cells with the supernatant of transfected cells

To test whether the reporter construct JFH1-hmAG can produce and release infectious virus particles, we inoculated naïve Huh-7.5.1 cells with the culture supernatant obtained from the transfected cells 30 days after transfection with JFH1-hmAG RNA. Two days after inoculation, NS5A-mAG signal was visualized in infected cells by fluorescence microscopy while not in uninfected cells (Fig. 2C). Immunostaining showed the same colocalization configuration of NS5A-mAG and Core proteins in inoculated cells (Fig. 2D) as in the transfected cells (Fig. 2B). Therefore, we considered that the new recombinant virus replicates in the same manner as the parental JFH1, even though NS5A was truncated by insertion of hmAG. Moreover, the RNA in cells and supernatants was considered to keep integrity without loss of the inserted mAG because all the RT-PCRs targeting the 5′UTR, NS3, and NS5A-hmAG junction regions yielded the products with predicted sizes (Fig. 3).

Taken altogether, we concluded that the JFH1-hmAG clone is infectious and replication-competent. In the transfected cells, JFH1-hmAG RNA produced NS5A-mAG/Core proteins, replicated, and released HCV particles that were infectious to Huh-7.5.1 cells. Though the culture supernatants of transfected cells at different time points were capable of infecting and re-infecting Huh-7.5.1 cells (data not shown), further studies seem necessary to

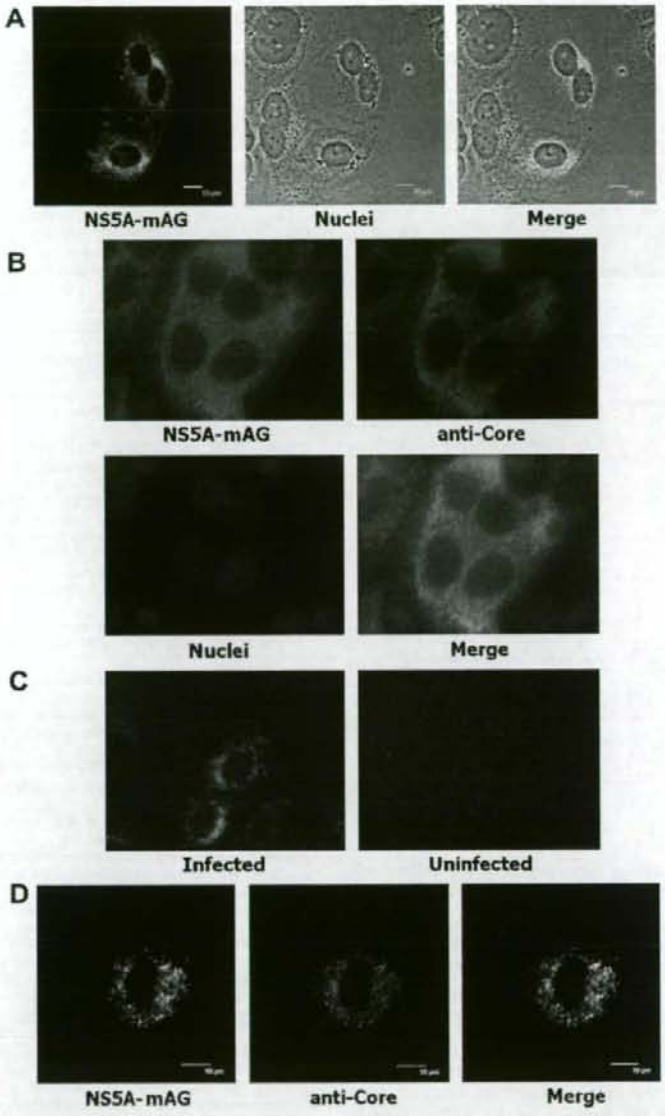

Fig. 2. Cell Images by fluorescence microscopy. (A) Huh-7.5.1 cells were analyzed by confocal microscopy 3 days after transfection with JFH1-hmAG RNA. The mAG emitted green signals. (B) Subcellular localization of NS5A-mAG and Core proteins in transfected cells. Huh-7.5.1 cells transfected with JFH1-hmAG RNA were grown in a 8-well chamber for 3 days. Cells were stained with monoclonal anti-Core mouse antibody and Alexa Fluor 594-conjugated donkey anti-mouse antibody. The localization patterns of NS5A-mAG and Core were shown in green and red, respectively. The merged images were also shown. Nuclei were stained with DAPI (blue). (C) NS5A-mAG was directly visualized in Huh-7.5.1 cells by fluorescence microscopy after inoculation with the culture supernatant obtained from the transfected cells 30 days after RNA transfection. (D) Subcellular localization of NS5A-mAG and Core protein in infected cells. NS5A-mAG and Core proteins were visualized 2 days after inoculation as described in (B).

determine the infectivity and integrity of JFH1-hmAG virus for a longer period, since genetic mutations frequently appeared in an persistent HCV infection in vitro [33].

Inhibition of JFH1-hmAG infection by interferon (IFN)

The current standard therapy to chronic hepatitis C includes IFN [34]. JFH1 replication has been found to be sensitive to IFN [2]. To test IFN-sensitivity of JFH1-hmAG, we examined the viral infection in the presence of IFNα. Huh-7.5.1 cells were pretreated for 12 h with IFNα and then were incubated with the culture supernatant containing JFH1-hmAG virus. Three days after infection, the levels of intracellular HCV RNA were determined by RT-qPCR (Fig. 4). IFNα pretreatment inhibited JFH1-hmAG RNA accumulation in a dose-dependent manner (Fig. 4). Thus, the results imply that JFH1-hmAG inherited IFN-sensitivity from JFH1 and that this new infection system is useful for studying mechanisms of IFN actions and viral resistance to IFNs.

In conclusion, we have developed a novel infectious HCV clone (JFH1-hmAG) containing *hmAG* in the NS5A region of the genome,

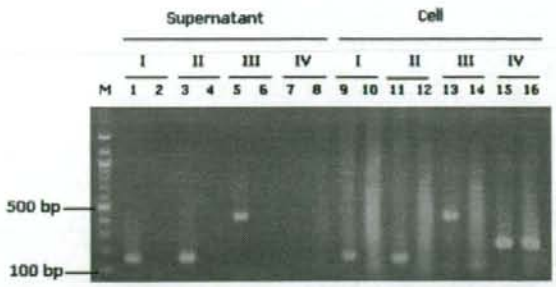

Fig. 3. Reverse transcription (RT) PCR. Huh-7.5.1 cells were inoculated with the supernatant containing JFH1-hmAG virus. Two days after infection, RNA was extracted from cell culture supernatant and from harvested cells. RT-PCRs targeting 5′UTR (group I), NS3 (group II), NS5A-hmAG junction (group III) regions in JFH1-hmAG genome were performed, respectively. RT-PCR targeting GAPDH (group IV) mRNA was also performed simultaneously as a control. Reactions with RNA extracted from culture supernatants (lanes 1, 3, 5, and 7) or cells (lanes 9, 11, 13, and 15) with infection, and from culture supernatants (lanes 2, 4, 6, and 8) or cells (lanes 10, 12, 14, and 16) without infection were shown, respectively.

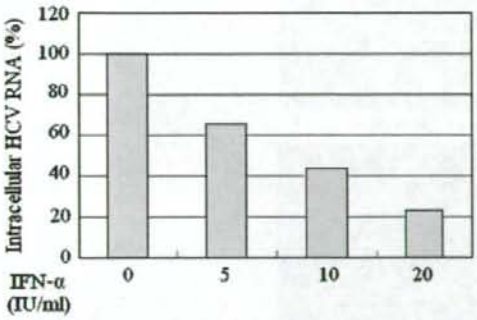

Fig. 4. Inhibition of JFH1-hmAG replication by interferon alpha (IFNα). Huh-7.5.1 cells in duplicate were treated with 0, 5, 10, and 20 U/ml. IFNα followed by incubation with the culture supernatant containing with JFH1-hmAG virus. Three days after infection, the relative numbers of intracellular HCV RNA molecules were determined by RT-qPCR (see Materials and methods). Each bar represents the mean number of intracellular HCV RNA molecules expressed as a percentage of that in the control infection without IFN pretreatment.

and have been able to readily observe living infected cells by green-emitting fluorescence. Its replication was restricted by IFNα in a dose-dependent manner. Our results suggested that this new recombinant virus replicated as properly as the parental JFH1 virus, and that this new reporter virus is useful in investigating the HCV biology and the anti-HCV action of IFNs. The JFH1-hmAG virus may provide us with a new system useful for readily screening anti-HCV drugs.

Acknowledgments

We are grateful to Drs. Takaji Wakita and Francis V. Chisari for pJFH1 and Huh-7.5.1, respectively. We thank Drs. Mitsue Hayashi, Zene Matsuda, and Kunito Yoshiike for discussion and encouragement.

W.H. was supported by China Postdoctoral Science Foundation funded project (No. 20070410154). This work was supported by the Program of Founding Research Centers for Emerging and Reemerging Infectious Diseases that was launched as a project commissioned by the Ministry of Education, Culture, Sports, Science and Technology (MEXT), Japan.

References

[1] T. Wakita, T. Pietschmann, T. Kato, T. Date, M. Miyamoto, Z. Zhao, K. Murthy, A. Habermann, H.G. Kräusslich, M. Mizokami, R. Bartenschlager, T.J. Liang, Production of infectious hepatitis C virus in tissue culture from a cloned viral genome, Nat. Med. 11 (2005) 791–796.
[2] J. Zhong, P. Gastaminza, G. Cheng, S. Kapadia, T. Kato, D.R. Burton, S.F. Wieland, S.L. Uprichard, T. Wakita, F.V. Chisari, Robust hepatitis C virus infection in vitro, Proc. Natl. Acad. Sci. USA 102 (2005) 9294–9299.
[3] B.D. Lindenbach, M.J. Evans, A.J. Syder, B. Wölk, T.L. Tellinghuisen, C.C. Liu, T. Maruyama, R.O. Hynes, D.R. Burton, J.A. McKeating, C.M. Rice, Complete replication of hepatitis C virus in cell culture, Science 309 (2005) 623–626.
[4] T. Pietschmann, A. Kaul, G. Koutsoudakis, A. Shavinskaya, S. Kallis, E. Steinmann, K. Abid, F. Negro, M. Dreux, F.L. Cosset, R. Bartenschlager, Construction and characterization of infectious intragenotypic and intergenotypic hepatitis C virus chimeras, Proc. Natl. Acad. Sci. USA 103 (2006) 7408–7413.
[5] M. Yi, Y. Ma, J. Yates, S.M. Lemon, Compensatory mutations in E1, p7, NS2, and NS3 enhance yields of cell culture-infectious intergenotypic chimeric hepatitis C virus, J. Virol. 81 (2007) 629–638.
[6] J.M. Gottwein, T.K. Scheel, A.M. Hoegh, J.B. Lademann, J. Eugen-Olsen, G. Lisby, J. Bukh, Robust hepatitis C genotype 3a cell culture releasing adapted intergenotypic 3a/2a (S52/JFH1) viruses, Gastroenterology 133 (2007) 1614–1626.
[7] T.K. Scheel, J.M. Gottwein, T.B. Jensen, J.C. Prentoe, A.M. Hoegh, H.J. Alter, J. Eugen-Olsen, J. Bukh, Development of JFH1-based cell culture systems for hepatitis C virus genotype 4a and evidence for cross-genotype neutralization, Proc. Natl. Acad. Sci. USA 105 (2008) 997–1002.
[8] M. Yi, R.A. Villanueva, D.L. Thomas, T. Wakita, S.M. Lemon, Production of infectious genotype 1a hepatitis C virus (Hutchinson strain) in cultured human hepatoma cells, Proc. Natl. Acad. Sci. USA 103 (2006) 2310–2315.
[9] R. Bartenschlager, T. Pietschmann, Efficient hepatitis C virus cell culture system: what a difference the host cell makes, Proc. Natl. Acad. Sci. USA 102 (2005) 9739–9740.
[10] R. Bartenschlager, S. Sparacio, Hepatitis C virus molecular clones and their replication capacity in vivo and in cell culture, Virus Res. 127 (2007) 195–207.
[11] R. Bartenschlager, Hepatitis C virus molecular clones: from cDNA to infectious virus particles in cell culture, Curr. Opin. Microbiol. 9 (2006) 416–422.
[12] J.M. Berke, D. Moradpour, Hepatitis C virus comes full circle: production of recombinant infectious virus in tissue culture, Hepatology 42 (2005) 1264–1269.
[13] J. Bukh, R.H. Purcell, A milestone for hepatitis C virus research: a virus generated in cell culture is fully viable in vivo, Proc. Natl. Acad. Sci. USA 103 (2006) 3500–3501.
[14] D. Moradpour, F. Penin, C.M. Rice, Replication of hepatitis C virus, Nat. Rev. Microbiol. 5 (2007) 453–463.
[15] M. Régeard, C. Lepère, M. Trotard, P. Gripon, J. Le Seyec, Recent contributions of in vitro models to our understanding of hepatitis C virus life cycle, FEBS J. 274 (2007) 4705–4718.
[16] P. Sheehy, B. Mullan, I. Moreau, E. Kenny-Walsh, F. Shanahan, M. Scallan, L.J. Fanning, In vitro replication models for the hepatitis C virus, J. Viral Hepat. 14 (2007) 2–10.
[17] T. Suzuki, H. Aizaki, K. Murakami, I. Shoji, T. Wakita, Molecular biology of hepatitis C virus, J. Gastroenterol. 42 (2007) 411–423.
[18] T.L. Tellinghuisen, M.J. Evans, T. von Hahn, S. You, C.M. Rice, Studying hepatitis C virus: making the best of a bad virus, J. Virol. 81 (2007) 8853–8867.
[19] M.B. Zeisel, T.F. Baumert, Production of infectious hepatitis C virus in tissue culture: a breakthrough for basic and applied research, J. Hepatol. 44 (2006) 436–439.
[20] M.P. Manns, G.R. Foster, J.K. Rockstroh, S. Zeuzem, F. Zoulim, M. Houghton, The way forward in HCV treatment—finding the right path, Nat. Rev. Drug Discov. 6 (2007) 991–1000.
[21] K. Moriishi, Y. Matsuura, Evaluation systems for anti-HCV drugs, Adv. Drug Deliv. Rev. 59 (2007) 1213–1221.
[22] J.M. Pawlotsky, S. Chevaliez, J.G. McHutchison, The hepatitis C virus life cycle as a target for new antiviral therapies, Gastroenterology 132 (2007) 1979–1998.
[23] S. Saito, T. Heller, M. Yoneda, H. Takahashi, A. Nakajima, J.T. Liang, Lifestyle-related diseases of the digestive system: a new in vitro model of hepatitis C virion production: application of basic research on hepatitis C virus to clinical medicine, J. Pharmacol. Sci. 105 (2007) 138–144.
[24] T. Wakita, HCV research and anti-HCV drug discovery: toward the next generation, Adv. Drug Deliv. Rev. 59 (2007) 1196–1199.
[25] C.S. Kim, J.H. Jung, T. Wakita, S.K. Yoon, S.K. Jang, Monitoring the antiviral effect of alpha interferon on individual cells, J. Virol. 81 (2007) 8814–8820.
[26] T. Schaller, N. Appel, G. Koutsoudakis, S. Kallis, V. Lohmann, T. Pietschmann, R. Bartenschlager, Analysis of hepatitis C virus superinfection exclusion by using novel fluorochrome gene-tagged viral genomes, J. Virol. 81 (2007) 4591–4603.
[27] D. Moradpour, M.J. Evans, R. Gosert, Z. Yuan, H.E. Blum, S.P. Goff, B.D. Lindenbach, C.M. Rice, Insertion of green fluorescent protein into nonstructural protein 5A allows direct visualization of functional hepatitis C virus replication complexes, J. Virol. 78 (2004) 7400–7409.

[28] S. Karasawa, T. Araki, M. Yamamoto-Hino, A. Miyawaki, A green-emitting fluorescent protein from Galaxeidae coral and its monomeric version for use in fluorescent labeling, J. Biol. Chem. 278 (2003) 34167–34171.
[29] C.N. Stewart Jr., Go with the glow: fluorescent proteins to light transgenic organisms, Trends Biotechnol. 24 (2006) 155–162.
[30] T. Kato, T. Date, A. Murayama, K. Morikawa, D. Akazawa, T. Wakita, Cell culture and infection system for hepatitis C virus, Nat. Protoc. 1 (2006) 2334–2339.
[31] S.B. Kapadia, A. Brideau-Andersen, F.V. Chisari, Interference of hepatitis C virus RNA replication by short interfering RNAs, Proc. Natl. Acad. Sci. USA 100 (2003) 2014–2018.
[32] T. Masaki, R. Suzuki, K. Murakami, H. Aizaki, K. Ishii, A. Murayama, T. Date, Y. Matsuura, T. Miyamura, T. Wakita, T. Suzuki, Interaction of hepatitis C virus nonstructural protein 5A with core protein is critical for the production of infectious virus particles, J. Virol. 82 (2008) 7964–7976.
[33] J. Zhong, P. Gastaminza, J. Chung, Z. Stamataki, M. Isogawa, G. Cheng, J.A. McKeating, F.V. Chisari, Persistent hepatitis C virus infection in vitro: coevolution of virus and host, J. Virol. 80 (2006) 11082–11093.
[34] R. De Francesco, G. Migliaccio, Challenges and successes in developing new therapies for hepatitis C, Nature 436 (2005) 953–960.

PROTEINS
STRUCTURE • FUNCTION • BIOINFORMATICS

STRUCTURE NOTE

Rhesus macaque: A tight homodimeric CD8αα

Lili Zong,[1,2] Yong Chen,[1,3,4] Hao Peng,[1] Feng Gao,[1] Aikichi Iwamoto,[3,5,6] and George F. Gao[1,3]*

[1] CAS Key Laboratory of Pathogenic Microbiology and Immunology (CASPMI), Institute of Microbiology, Chinese Academy of Sciences (CAS), Beijing 100101, China

[2] Department of Obstetrics and Gynaecology, Zhujiang Hospital, Nanfang Medical University, Guangzhou 510280, China

[3] China-Japan Joint Laboratory of Molecular Immunology and Molecular Microbiology, Institute of Microbiology, Chinese Academy of Sciences (CAS), Beijing 100101, China

[4] College of Life Sciences, Graduate University, Chinese Academy of Sciences (GUCAS), Beijing 100049, China

[5] Research Center for Asian Infectious Diseases, The Institute of Medical Science, The University of Tokyo, Tokyo, Japan

[6] Division of Infectious Diseases, Advanced Clinical Research Center, The Institute of Medical Science, The University of Tokyo, Tokyo, Japan

Key words: rhesus macaque; crystal structure; MHC binding; CD8; dimer; HIV; vaccine.

INTRODUCTION

Simian immunodeficiency virus (SIV) infection of rhesus macaque (*macaca mulatta*) is widely used as an animal model for human immunodeficiency virus (HIV) infection[1–3] as well as other human diseases. It is known that the host cytotoxic T lymphocyte (CTL) responses provide powerful protection against HIV infection, and CTL-based immunization is currently believed to be the most promising approach toward vaccine development.[4]

As a coreceptor of T cell receptor (TCR) on the surface of CTLs, CD8 molecules stabilize the interaction of the TCR with major histocompatibility complex (MHC) by binding to the MHC class I (MHCI) molecule on the surface of antigen-presenting cells. In the absence of CD8 interaction, MHCI-restricted immune responses are hampered.[5] In addition, recent data indicate that CD8 has the ability to bind to a nonclassical MHC class I-like molecule, TL antigen, independently of TCR and CD3, expanding the function of CD8 further to an immunomodulator.[6–8] Moreover, soluble forms of CD8 can disrupt activation of some T cell clones with higher efficacy than anti-CD8 antibodies.[9,10]

In both human and mouse, the functions of CD8 involved in immune responses have been extensively studied.[11,12] The crystal structures of the human HLA-A*0201-CD8αα complex,[13,14] murine MHC H-2K^b-CD8αα complex,[15] TL antigen-CD8αα complex,[16] and the murine CD8αβ heterodimer[17] have been solved. For macaque monkeys, however, little is known on the structures of the CTL-related molecules (e.g., TCR, MHC, and CD8). Only the structure of MHC allele Mamu-A*01 has been recently solved in our laboratory.[18]

In this article, we present the crystal structure of rhesus macaque CD8αα (rCD8αα) homodimer and discuss the relatedness and uniqueness of rCD8αα structure with that of human/mouse CD8αα homodimer. Strikingly, with two Thr43 residues in C–C′ loop, rCD8αα shows a unique extra hydrogen bond in the homodimeric interface indicating a tighter homodimeric interaction.

Grant sponsor: Ministry of Science and Technology (MOST), China (Basic Research Program 973); Grant number: 2006CB504204; Grant sponsor: National Natural Science Foundation (NSFC), China; Grant number: 30671903; Grant sponsor: Chinese Academy of Sciences (CAS, Knowledge Innovation Project); Grant number: KSCX2-SW-227; Grant sponsor: NSFC; Grant number: 30525010; Grant sponsor: Postdoctoral Fund of China; Grant number: 20070410649; Grant sponsor: Japan Ministry of Education, Culture, Sports, Science and Technology (MEXT, The China-Japan Joint Laboratory of Molecular Immunology and Molecular Microbiology).

Lili Zong and Yong Chen contributed equally to this work.

*Correspondence to: George F. Gao, Center for Molecular Immunology, Institute of Microbiology, Chinese Academy of Sciences (CAS), Datun Road, ChaoYang District, Beijing 100101, China. E-mail: gaof@im.ac.cn

Received 28 September 2008; Revised 10 November 2008; Accepted 12 November 2008

Published online 19 November 2008 in Wiley InterScience (www.interscience.wiley.com). DOI: 10.1002/prot.22331

MATERIALS AND METHODS

Expression and purification of rCD8αα homodimer

Rhesus macaque CD8 (rCD8) alpha chain nucleotides covering amino acids 1–120 of the ectodomain were synthesized based on the sequence of Indian origin rhesus (GeneBank ID: 698329). Inclusion bodies of rCD8α were prepared, and rCD8αα homodimer was renatured and purified by using the protocols described earlier.[13,14]

Crystallization, data collection, and processing

All crystallization attempts were performed at 18°C by the hanging drop vapor diffusion method. Ideal rCD8αα crystals grew from a 1:1 mixture of the protein solution (10 mg/mL) with crystallization reagent of 0.05*M* potassium phosphate monobasic, 20% w/v polyethylene glycol 8000. Data were collected using a Rigaku MicroMax007 rotating-anode X-ray generator (Cu Kα; λ = 1.5418 Å) equipped with an R-AXIS VII++ image-plate detector. Data were processed and scaled using HKL2000.[19]

Structure solution, refinement, and analysis

Data were analyzed by molecular replacement[20] using Molrep in the CCP4 package,[21] taking human CD8αα as the search probe (PDB code: 1AKJ).[14] Final rounds of refinement resulted in a final Rcryst of 21.3% (R_{free} = 25.7%) for all data between 35.0 and 2.20 Å.

Buried surface areas were calculated using SURFACE[21] with a 1.4 Å probe radius. The PyMOL Molecular Graphics System (DeLano Scientific, http://www.pymol.org) was used to prepare figures. Geometry of the refined structure was validated according to Ramachandran plot criteria.[22] The data collection and refinement statistics of the structure are shown in Table I.

Accession number

Atomic coordinates of rhesus macaque CD8αα homodimer have been deposited in the Protein Data Bank (PDB, http://www.rcsb.org/pdb) under accession code: 2Q3A.

Table I
X-Ray Diffraction Data Processing and Refinement Statistics

Data collecting	
Space group	$P2_12_12_1$
Unit cell dimensions (*a*, *b*, *c*)	46.54, 56.26, 82.31
Unit cell dimensions (α, β, γ)	90.00, 90.00, 90.00
Resolution range (Å)	40.00–2.20 (2.32–2.20)[a]
Total number of reflections	138,752
Number of unique reflections	17,807
Number of molecule in the asymmetric unit	2
Average redundancy	6.60 (5.90)
Completeness (%)	99.6 (100.0)
R_{merge} (%)	9.6 (29.5)
I/σ	12.8 (5.7)
Refinement	
Resolution (Å)	35.85–2.20
R-factor (%)	21.3
R_{free}[b] (%)	25.7
RMS deviations from restraint target values:	
Bond lengths (Å)	0.006
Bond angles (°)	1.33
Ramachandran plot Quality:	
Residues in most favored regions	165 [84.2%]
Residues in additional allowed	27 [13.8%]
Residues in generously allowed	4 [2.0%]
Residues in disallowed regions	0 [0%]

[a]Values in parentheses are given for the highest resolution shell.
[b]R_{free} is calculated over reflections in a test set (5%) not included in atomic refinement.

RESULTS AND DISCUSSION

Overall structure of rhesus macaque CD8αα homodimer

The crystals contained two CD8αα molecules as a dimer in a hand-shaking mode per crystallographic asymmetric unit. Belonging to the V set of Ig folds,[14] the overall structure comparison of rCD8αα homodimer with the human counterpart is shown in Figure 1(A). Each CD8α molecule is primarily composed of β structure arranged into two antiparallel β sheets. Short regions of 3_{10} helix are found between the E and F strands, which are not commonly found in CD8β molecules.

All residues corresponding to the HLA-A2-CD8αα interface remain the same in MHC Mamu-A*01 and rCD8αα.[18] The interaction of HLA-CD8 is mainly based on charge complementarity and exhibits relatively low affinity (KD = 100–223 μ*M*) and rapid kinetics.[8,23] The molecular surfaces of Mamu-A*01 and rCD8αα show similar complementarities (data not shown), indicating their interaction.

Structural comparison of rhesus macaque with human or murine CD8αα homodimer

Superposition of the final structure of rCD8αα dimer shows closer resemblance to human CD8αα homodimer (1AKJ, in complex with HLA-A2)[14] than to murine CD8αα (mCD8αα) (1BQH, in complex with Kd)[15] [Fig. 1(A,B)]. Root mean square deviation (RMSD) of rCD8αα and hCD8αα dimer results in 0.831 E for all Cα atoms, which is much smaller than that of rCD8αα with mCD8 dimer of 1.634 E.

The comparison of r/h/m CD8αα reveals some differences in loop regions, especially in complementarity